1-6-2017

Applications of Monolithic Capillary Electrochromatography (CEC): Method Development and Quantitation of Metabolites in Prostate Tissue and Insights into Chiral Recognition Mechanism

Yang Lu

APPLICATIONS OF MONOLITHIC CAPILLARY ELECTROCHROMATOGRAPHY (CEC): METHOD DEVELOPMENT AND QUANTITATION OF METABOLITES IN PROSTATE TISSUE AND INSIGHTS INTO CHIRAL RECOGNITION MECHANISM

by

Yang Lu

Under the Direction of Shahab A. Shamsi, PhD

ABSTRACT

Capillary electrochromatography (CEC) is a major capillary electrophoresis (CE) mode that have been interfaced to mass spectrometry (MS) for sensitive and selective analysis of chiral compounds. This research expands CEC applications in cancer biomarker and chiral CE analysis. Chapter 1 is a review of liquid chromatography-mass spectrometry (LC/MS), gas chromatography-mass spectrometry (GC/MS), and capillary electrophoresis mass spectrometry (CE/MS) for analysis of metabolites in prostate cancer diagnostics and therapies. In this chapter, a literature survey was performed within the databases PubMed, 4 Caplus/Webline and Web of Sciences. A total 17 studies reporting on various analytical platforms for metabolite identification in prostate cancer research, which often include case-control comparison were identified and reviewed. Chapter 2 described the analysis of metabolite biomarkers in prostate cancer tissues by capillary electrochromatography mass spectrometry. In this chapter, a capillary CEC–MS/MS method was developed for the simultaneous determination and separation of eight proofs of concept (POC)

metabolites (betaine, malate, proline, N-acetyl aspartate, N-acetylglucosamine, uracil, xanthine, and alanine) as potential prostate cancer diagnostic markers. A polymeric monolith column with a hydrophilic crosslinker and strong anion-exchange mixed-mode has been fabricated by an in situ copolymerization of vinyl benzyl trimethylammonium chloride, and bisphenol A glycerolate dimethacrylate (BisGMA) in the presence of methanol and dodecyl alcohol as porogens and AIBN as initiator. After CEC separation, samples were analyzed by a triple–quadrupole mass spectrometer operated in positive ion mode. After optimization, the data showed that the CEC-MS/MS method using monolithic column achieved a much better chromatographic selectivity compared to coated columns and increased sensitivity than bare fused silica column The effect of mobile phase pH, ACN percentage and additive were studies. Under the optimum mobile phase conditions, this method was carried out to separate and detect eight metabolites in the biopsy sample. The LOD for the metabolites is between 50nM-100nM. This method has successfully used to examine patients' prostate cancer with an accuracy of 95%. Chapter 3 demonstrates Insights into Chiral Recognition Mechanisms in CEC using linear salvation energy relationship. By varying the linker (amide and carbamate), head group (alanine, leucine, and valine) and chain length (C8, C10 and C12) of the amino acid bound surfactants; monolithic column was made to ultimately understand the factors governing chiral stationary solid phase. Through the comparison of system parameters, we can see that surfactant head group, linker and chain length affect the separation of achiral and chiral compounds. Also, with the same type surfactant, data was presented to show how the trend of LSER parameters and how it affects separation between in CEC. This study showed the predictive capability of LSER to understand the aforementioned intermolecular processes controlling retention and by doing so, be able to quantitatively predict the experimental conditions to achieve an acceptable chiral separation.

INDEX WORDS: Capillary electrochromatography (CEC), Prostate cancer, Metabolites, Cancer biomarkers, Chiral separation, Mass spectrometry, Chiral monolithic stationary phases, Multivariate design

APPLICATIONS OF MONOLITHIC CAPILLARY ELECTROCHROMATOGRAPHY (CEC): METHOD DEVELOPMENT AND QUANTITATION OF METABOLITES IN PROSTATE TISSUEAND INSIGHTS INTO CHIRAL RECOGNITION MECHANISM

by

Yang Lu

A Dissertation Submitted in Partial Fulfillment of the Requirements for the Degree of

Doctor of Philosophy

in the College of Arts and Sciences

Georgia State University

2016

APPLICATIONS OF MONOLITHIC CAPILLARY ELECTROCHROMATOGRAPHY (CEC): METHOD DEVELOPMENT AND QUANTITATION OF METABOLITES IN PROSTATE TISSUEAND INSIGHTS INTO CHIRAL RECOGNITION MECHANISM

by

Yang Lu

Committee Chair: Shahab A. Shamsi

Committee: George Peng Wang

Ming Luo

Electronic Version Approved:

Office of Graduate Studies

College of Arts and Sciences

Georgia State University

August 2016

DEDICATION

To my family

ACKNOWLEDGEMENTS

I would like to sincerely thank my advisor Dr. Shahab A. Shamsi for his thoughtful and patient guidance during my graduate studies at Georgia State University. I would also like to thank my dissertation committee member Drs. George Peng Wang and Ming Luo for their help in writing this dissertation and throughout my whole graduate projects. Additionally, I am very grateful for the friendship and help from all the colleagues in my research group, namely Drs. Jun He, William Bragg, Xiaochun Wang, Yijin Liu., Ms. Ferdoushi Akter and Mr. A S M Mojibur Rahaman Chawdhury. I also owe many thanks to the collaborators in my dissertation projects, especially Dr. Robert Simmons for the help with SEM imaging, Dr. Dean Troyer for the help with prostate cancer biopsy samples.

Finally, and most importantly, I would like to thank my husband Along and my parents. Without their help, I cannot finish my dissertation.

TABLE OF CONTENTS

LIST OF TABLES

LIST OF FIGURES

CHAPTER 1: Review of Liquid Chromatography-Mass Spectrometry (LC/MS), Gas Chromatography-Mass Spectrometry (GC/MS) and Capillary Electrophoresis Mass Spectrometry (CE/MS) for Analysis of Metabolites in Prostate Cancer Diagnostics and Therapies

1.1 Abstract

In this introductory chapter, an overview is presented on a number of important aspects related to the analysis of metabolites in prostate cancer research. A literature survey was performed within the databases PubMed, 4 Caplus/Webline and Web of Sciences. A total 17 studies reporting on various analytical platforms for metabolite identification in prostate cancer research, which often include case-control comparison were identified and reviewed. More particularly, this chapter summarizes the present situation with respect to the review of chromatography-mass spectrometry platforms, sample type, study type and the type of mass spectrometers used in prostate cancer research. Despite current challenges, metabolomics has the potential to evolve into a standard tool in prostate cancer.

1.2 Introduction

1.2.1 Metabolism, Metabolites, Metabolome and Metabolomics

Metabolism is a term used to describe a set of chemical reactions of the living organism to sustain life. A series of enzyme participate in these reactions to allow cells to grow and reproduce. There are two subdivisions of metabolism: catabolism and anabolism. Catabolism is the breakdown procedure of large molecules to obtain energy (e.g., hydrolysis reaction and cellular respiration). Conversion from starch to glucose involves hydrolysis and energy are released in the reaction. Anabolism, which is a reverse of catabolism, refers to constructive metabolism, in which simpler

molecules such as various cell components can be combined to form more complex molecules such as proteins and nucleic acids resulting in energy storage in these molecules.

1.2.2 Metabolites: Properties and Function of Metabolite

Metabolites are a catalytic product of enzyme reactions, which occur inside the cell. Six major factors are considered when classifying a substance as a metabolite. These six factors in metabolite classification include: (a) metabolite formation occurs within the cell (intracellularly); (b) metabolites rearrange and react with enzymes; (c) metabolic product must proceed to form another species in a subsequent reactions, (d) metabolite have a well-defined half-life and they do not store in cells; (e) metabolites serves as a regulator controlling the speed of many metabolisms; (f) metabolites serve important biological functions in the cell. Metabolites are also termed as intermediates (intermediate metabolite) and products of metabolism (final metabolite). When metabolites usually refer to the small molecule, they are defined as primary or secondary metabolites. Primary metabolites are directly involved in normal cell growth, development, and reproduction. (e.g., amino acids metabolism). On the other hand, secondary metabolites are not directly involved in these processes, but may have a long-term effect on human survivability.

The enzyme is essential for metabolic reactions because the presence of enzyme allow a thermodynamically difficult reaction to occur when coupled to another spontaneous reaction. One example, which shows the potential of the enzyme is the energy generated from ATP hydrolysis to drive another chemical reaction. Metabolism of an organism determines which substances for this organism are nutritious and which are poisonous. For example, hydrogen sulfide serves as nutrition to some prokaryotes, but the same chemical is toxic to animals.[1] The speed of metabolism

reactions, known as the term "metabolic rate," also affects an organism food demand. For example, faster the ATP to ADP conversion rate, the higher will be food demand.

1.2.3 Characteristics of Metabolism

Metabolism has a very useful characteristic, i.e., the basic metabolic pathways are similar between different species. For example, citric acid (also known as tricarboxylic acid (TCA), is present in all organisms, which may be unicellular organisms such as tiny bacteria or even huge multicellular organisms such as elephants.[2] Such metabolic similarity is due to the high efficiency associated with metabolic pathways, and their early appearance in the evolutionary history.[3,4] There are numerous metabolic pathways. The most important metabolic processes in human includes: citric acid cycle (Krebs' cycle), oxidative phosphorylation, pentose phosphate pathway, urea cycle, fatty acid β-oxidation, and gluconeogenesis.

The metabolome is a sum of all small molecules found in a biological sample, e.g., cell, tissue, tissue extract, biofluid, organs or even an organism. Essentially, metabolome involves the interaction of an organism genome with its environment. Therefore, an organism metabolome is a good model of its phenotype, which is a product of genotype and its environment. In different species, metabolomes are different. Even in the same species, metabolome differs from each other in different organ and tissue. Metabolome database such as Human Metabolome Database (HMDB)[5] and Yeast Metabolome Database (YMDB)[6] are widely used for metabolite search.

Metabolomics is a rapidly emerging omics in systems biology involving studies of an entire set of metabolites found in cells, tissue or the entire organism. The metabolites are first identified and detected with analytical technologies. Next, a systematic study is performed to quantitate and analyze the concentration of as many metabolites in a biological sample as possible. The term

metabolomics was first coined by Professor Jeremy Nicholson at Imperial College London in 1999.[7] After the rapid development, metabolomics is now related to a number of areas, such as disease diagnosis,[8] pharmaceutical research and development, nutrition, food science, drugs science, environmental science, botany and human health care.

Metabolite analysis has been used for many decades in disease diagnosis since Sir Archibald Garrod first links metabolism with human disease.[9-13] While other –omics, such as transcriptomic and proteomics, are well known for their important role in diagnostic and treatment of cancer and other diseases, metabolomics is also attracting more and more attention because of its high sensitivity to diet, stress and environmental related physiological changes. In transcriptomic and proteomics, the blueprint of tens of more than ten thousand targets is measured to monitor the organism functions. However, the metabolomic study is less time consuming because the smallest domain (only ~5000 metabolites in metabolism pathways of living organs) compared to other -omics.[14,15] Metabolomics is promising because it involves simple sample preparation procedure and ease of data comparison among different conditions.[7] In this introduction to dissertation chapter, the application of metabolomics in the diagnosis of prostate cancer is discussed. For prostate cancer, there is an urgent need to identify reliable biomarkers as a diagnostic tool for effective therapy design.

1.3 Identification of Studies in Prostate Cancer

To better understand **metabolomics** role for prostate cancer, four databases (PubMed, web of Science and CAPLUS/EDLINE) were searched with the following keywords "'Metabolomics' AND 'Prostate Cancer'" AND "'CE/MS', "'Metabolomics' AND '' Prostate Cancer AND 'GC/MS'", "'Metabolomics' AND 'Prostate Cancer' AND 'LC/MS'" from 2012 to 2016. Flow

charts for the review selection process for metabolites involved in the prostate is shown in Figure 1.1. We included only studies involving separations [gas chromatography (GC), high-performance liquid chromatography (HPLC)/ultrahigh pressure liquid chromatography (UPLC) or capillary electrophoresis (CE) coupled to mass spectrometry (MS) and approaches using only NMR, UV-98 Vis or (MS) were excluded. In addition, only discussions on human plasma, urine, CSF or tissue are included in this review. All duplicate findings were removed. Only papers reported in the English language are included in this review.

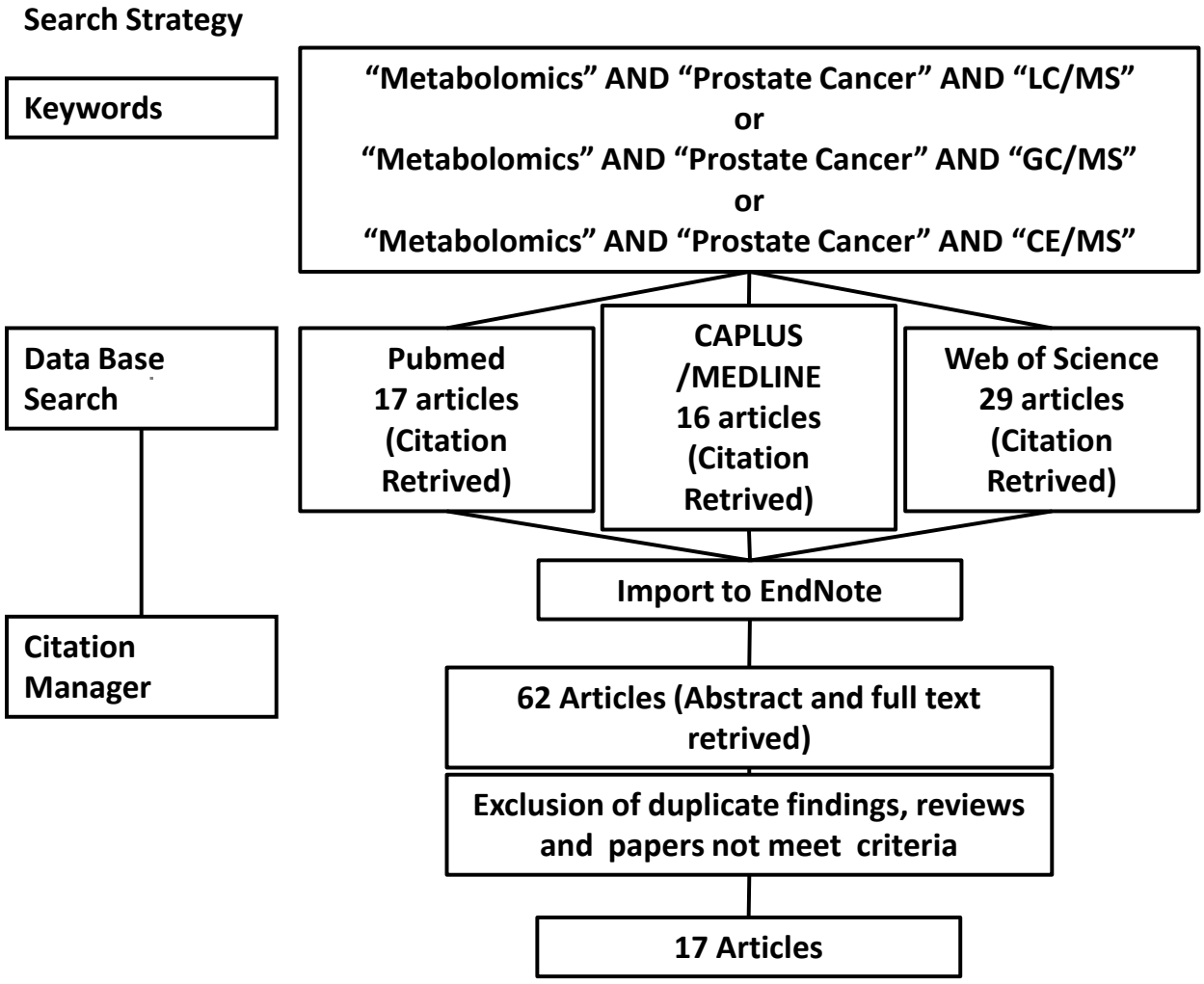

Figure 1.1 Schematic overview of the search strategy for metabolites in prostate cancer and neurological disease.

In total, 17 papers (as listed in Table. 1.1) were reviewed. The information (i.e., sample types, study types and analytical platforms) is illustrated in Figures 1.2- 1.5 and each of these topics are discussed below.

Table 1.1 Selected works published during the last 10 years regarding biomarkers of prostate cancer by LC or CE coupled to MS using a metabolomics approach.

Study	Disease type	Method	Sample	Metabolites pathway	Study type
Brown 2012[41]	Kidney and prostate cancer tumor	UPLC-LTQ-MS/MS	Tissue	amino acids, peptides, carbohydrates, lipids, nucleotides, cofactors, xenobiotics	Tissue profiling
Kapoore 2015[42]	Cancer	GC-q-MS	Tissue	amino acids, glucose, fatty acids and nucleotides	Metabolomics for therapy monitoring
Hu 2013[43]	prostate cancer	GC-ITQ-MS/MS	Tissue	amino acids, glucose, nucleotides and TCA cycle metabolites	Tissue profiling
Tripathi 2013	Bladder Cancer and Benign Disease	GC- MS*	Tissue	Amino acids	Tissue profiling
Brockmoeller 2012[44]	Breast Cancer	GC-TOF-MS	Tissue	sn-glycerol-3-phosphate	Tissue profiling
Liu 2015[45]	Prostate Cancer	UPLC-QqQ-MS/MS	Tissue	crucial steroidogenic enzymes-AKR1C3	Metabolomics for case-control comparison
McGinnis 2013[40]	prostate cancer	UPLC-qTOF-MS	Tissue	siRNAs	Method Development
Troyer 2013[46]	prostate cancer	LC- MS*	Tissue	Alanine, betaine, cysteine, malate, N-acetylaspartate, N-acetylglucosamine, proline, uracil, xanthine	Method Development

Study	Disease type	Method	Sample	Metabolites pathway	Study type
Huang 2014[47]	prostate cancer	LC-QTOF-MS	Serum	cholesterol metabolic and mitogen-activated protein kinase signaling pathway	Metabolomics for therapy monitoring
Kami 2012[39]	lung and prostate tumor	CE-TOF-MS	Tissue	lactate, tricarboxylic acid (TCA) cycle intermediates, and amino acids	Tissue profiling
Nacoulma 2013[48]	Lung, breast and prostate tumor	GC-ITQ-MS	Tissue	Cembrene derivatives, Incensole derivatives, glucose, amino acids, organic and phenolic acids	Metabolomics for case-control comparison
Wei 2013[49]	Breast cancer	LC-QTOF-MS/MS	Serum	threonine, isoleucine, glutamine and linolenic acid	Metabolomics for therapy monitoring
Sampson 2013[31]	Prostate, Lung, Colorectal, and Ovarian Cancer	LC-LIT-MS and GC-MS*	Plasma	amino acids, carbohydrates, fatty acids, androgens, and xenobiotics	Metabolomics for patient prognosis
Cross 2014[20]	Colorectal, Prostate, Lung, Colorectal, and Ovarian Cancer	GC-MS*	Serum	amino acids, carbohydrates, fatty acids, androgens, and xenobiotics	Metabolomics for patient prognosis
Li 2015[50]	Prostate cancer	LC-LTQ-Orbitrap-MS/MS	Tissue	Multiple peptides derived from osteopontin	Metabolomics for patient prognosis
Guertin 2015[51]	Prostate, Lung, Colorectal, and Ovarian Cancer	UPLC-MS/MS and GC-MS*	Serum	Caffeine-related metabolites	Metabolomics for case-control comparison

Study	Disease type	Method	Sample	Metabolites pathway	Study type
Struck-Lewicka 2016[52]	Prostate cancer	LC-TOF-MS and GC-QqQ-MS/MS	Urine	Urea and tricarboxylic acid cycle, amino acid and purine metabolism	Metabolic fingerprintin

.

1.4 Role of Metabolomics in Prostate Cancer

As mentioned earlier, metabolomics requires analysis of metabolite concentration change in a biological sample related to a certain disease. The biological specimen used in prostate cancer diagnostic includes urine, blood, and human tissues; each contains a different type of metabolites pathway information. A successful clinicopathologic and demographic evaluation should consider the ease of sample handling and preparation, patient demographic, instrumentation and method reliability. For therapy monitoring or case-control comparison studies, a larger sample pool is required, and the sample number is usually above 100. No significant difference should be observed among the patients in terms of median age, comorbid conditions and menopausal status. One typical case is a recent report with a list of over 110 metabolites in prostate cancer tissues.[16] In this study, the sample collection, sample preparation, and metabolite extraction were described, and the metabolites belong to different pathways and across all major biomedical classes such as amino acid metabolism (proline, cysteine, alanine, histidine, lysine, leucine, serine, N-acetyl-aspartyl-glutamate (NAG), betaine, N-acetyl aspartate (NAA) etc.), energy metabolism (malic, succinate, phosphate etc.), carbonhydrate (glucose, ribose etc.), lipid (choline, cartinine, glycerol etc), nucleotide (uracil, uidine, xanthine etc), cofactors and vitamins (alpha-tocopherol and panothenate). The authors applied the histology, metabolomic profiling, and statistical analysis to develop and validate the method with GC-MS and LC-MS in a single core needle biopsy to aid the prostate cancer diagnosis. The list of metabolites and pathways are shown in Table 1.2. In the next sub-sections, some critical aspects of prostate cancer research such as sample types, study types, analytical platforms and MS analyzers will be discussed detailed based on the literature survey.

Table 1.2 Metabolites in the sub pathways showing significant difference between cancer tumor and benign prostate samples.[16]

Sub Pathway	Biomedical
Alanine and aspartate metabolism	aspartate, alanine
Benzoate metabolism	benzoate, 2-aminobutyrate
Carnitine metabolism	3-dehydrocarnitine, acetylcarnitine, carnitine, deoxycarnitine
Cysteine, methionine, SAM, taurine metabolism	Cysteine, cystine, methionine, S-adenosylhomocysteine (SAH)
Fatty acid metabolism	docosapentaenoate (n3 DPA; 22:5n3), docosapentaenoate (n6 DPA; 22:5n6), butyrylcarnitine, propionylcarnitine, 4-hydroxybutyrate (GHB)
gamma-glutamyl	gamma-glutamylglutamate, gamma-glutamylglutamine
Glutamate metabolism	N-acetyl-aspartyl-glutamate (NAAG), glutamate
Glutathione metabolism	5-oxoproline, cysteine-glutathione disulfide, choline, ethanolamine, glycerol
Glycine, serine and threonine metabolism	Betaine, glycine, serine, threonine
Glycolysis, gluconeogenesis, pyruvate metabolism	glucose 1-phosphate, glucose
Histidine metabolism	Histidine
Krebs cycle	Fumarate, malate, succinate
Long chain fatty acid	dihomo-linoleate (20:2n6), eicosenoate (20:1n9 or 11), myristoleate (14:1n5), oleate (18:1n9)

Sub Pathway	Biomedical
Lysine metabolism	2-aminoadipate, lysine
Lysolipid	1-arachidonoylglycerophosphoethanolamine, 1-rachidonoylglycerophosphoinositol, 1-linoleoylglycerophosphoethanolamine, 1-oleoylglycerophosphoethanolamine, 1-leoylglycerophosphoinositol, 1-oleoylglycerophosphoserine, 1-almitoylglycerophosphoinositol, 1-stearoylglycerophosphoethanolamine, 1-tearoylglycerophosphoinositol, 2-oleoylglycerophosphoethanolamine, 2-almitoylglycerophosphoethanolamine
Medium chain fatty acid	caprylate (8:0)
Nucleotide sugars, pentose metabolism	ribose
Pantothenate and CoA metabolism	pantothenate
Phenylalanine & tyrosine metabolism	Phenylalanine, tyrosine
Purine and pyrimidine metabolism	methylphosphate
Purine metabolism	Hypoxanthine, inosine, xanthine, xanthosine, adenine, guanosine
Pyrimidine metabolism	Cytidine, pseudouridine, uracil, uridine
Urea cycle; arginine-, proline-, metabolism	Arginine, ornithine, proline, trans-4-hydroxyproline
Tryptophan metabolism	Tryptophan
Valine, leucine and isoleucine metabolism	valine

1.4.1 Sample Type Investigated for Prostate Cancer

A total of 17 papers were found in the metabolites analysis for prostate cancer. A pie diagram showing the distribution of sample type investigated for prostate cancer is shown in Figure 1.2. The most common sample assessed is tissue sample from tumor biopsy (11, 65%) followed by the traditional clinical sample, such as serum, plasma (total 5 studies, 29%), and urine (1 studies, 6%).

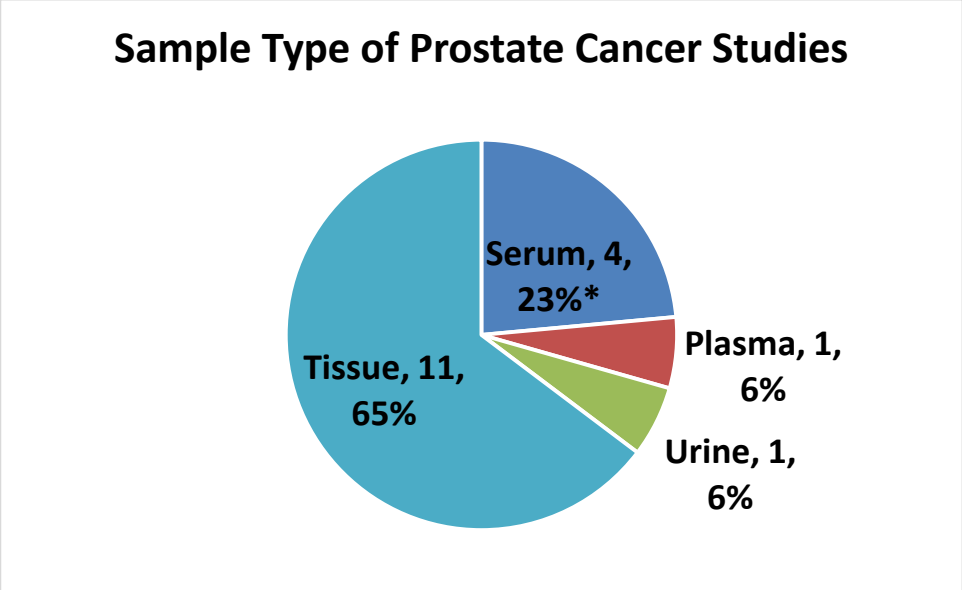

Figure 1.2 Pie diagram illustrating the study types used in prostate cancer. The number and percentage followed the name of the sample type represent the number of studies and the percentage in our study pool. The same style is employed for other pie charts shown in Figure 1.3-1.5.

Among all sample types, urine requires the least sample preparation (only centrifuge and dilution)[17]. In other samples types like tissue and CSF, protein needs to be removed before analysis. However, since metabolites concentration could be easily diluted or concentrated in a urine sample (sweating, drinking water, etc.), urine is not the best choices in most cases.

Whole blood, serum, and plasma are the second most routine specimen for prostate cancer. The concentration of metabolites in that sample can be related to pharmacological effect and due to

different metabolite profiles; In addition, whole blood, serum, and plasma could be used to monitor parent metabolites. [18-22]

Sample preparation for the solid sample is more difficult than the liquid samples. For examples, to liberate metabolites from complicated membranes and large molecules, tissue samples must be sliced with mechanical devices and extract with certain solvent. Moreover, one need to take extra care to avoid the leakage of metabolites from other biofluid sources (blood).[16,23-26] Nevertheless, as tissue sample could provide the widest range of metabolites profiling, the tissue sample is most widely used in the prostate cancer metabolomic analysis.

1.4.2 Study Types Investigated for Prostate Cancer

Pie chart with different study types distribution is shown in Figure 1.3. Five studies in tissue profiling are reported, and this accounts for 29% in the prostate cancer metabolomic study, which means the metabolism in prostate cancer is still not well understood, and new metabolic pathway are involved in either the disease pathology or treatment.[27] Furthermore, metabolites for therapy monitoring and patient prognosis are second most common study types in prostate cancer studies (18%) because the stronger demand for early diagnosis and treatment of prostate cancer. Metabolomics for case-control comparison is the third most common study types (3, 17%). In this last category, instead of independent validation, relative sample concentration change is employed.[20,26,28-32] Thus, case-control studies will give a clue on the future potential of metabolites use as an early diagnostic tool for prostate cancer. Fewer studies (1, 12%) are discussed in method development, and most of the studies are not quantitative enough due to the sample type and pathway complexity.

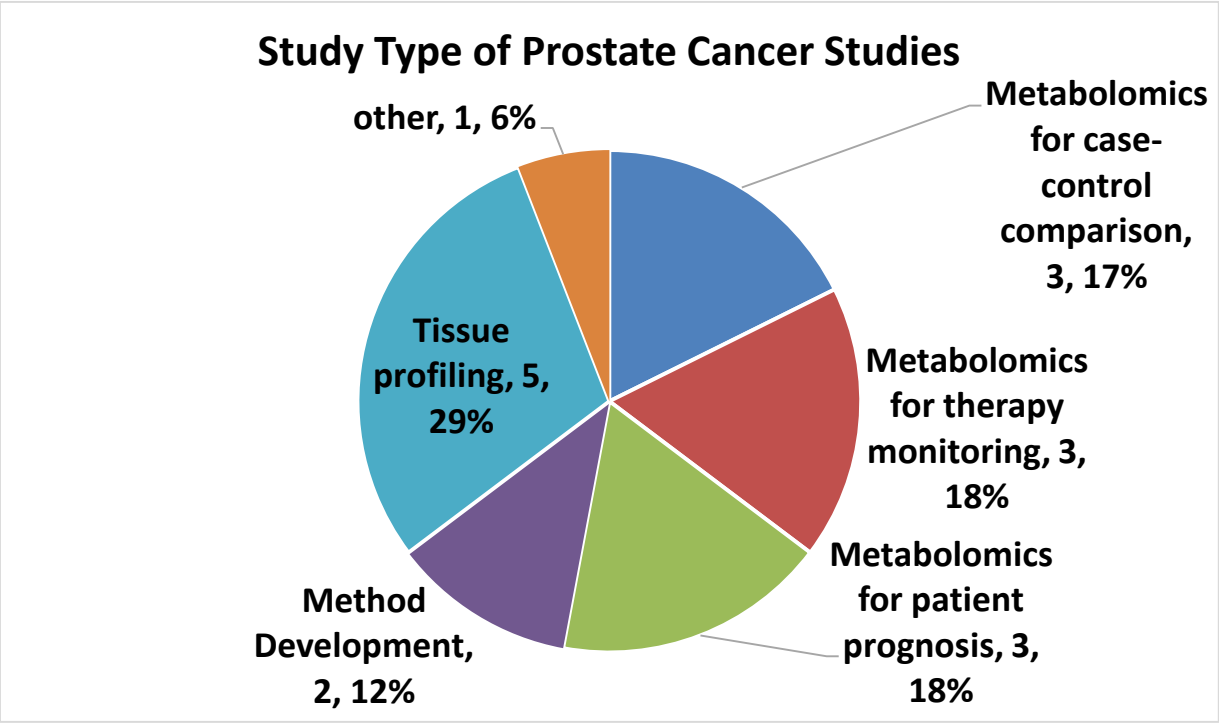

Figure 1.3 Pie diagram illustrating types of a biological sample used for prostate cancer studies. The number and percentage followed the name of the study type represent the number of studies and the percentage in our study pool.

1.4.3 Analytical Platforms based on GC/MS, LC/MS, and CE/MS for Prostate Cancer

To achieve a better understanding of metabolomic in prostate cancer, multiple analytical platforms have been employed, and the distribution for each platform is shown in Figure 1.4. Gas chromatography-MS (GC/MS) is a traditional method of choice and is exclusively studied due to its robustness and low ion suppression of mass spectrometer (e.g., single quadrupole).

GC/MS is widely used in prostate cancer metabolomic study (6, 35%) of both volatile and non-volatile analytes following derivatization.[16,22,25,33-35] Given the excellent selectivity and repeatability, modern GC/MS is an ideal tool for complex metabolic samples. However, it should be noted that only fewer metabolites can be detected by GC-MS due to the difficulty associated with derivatization of polar compounds.

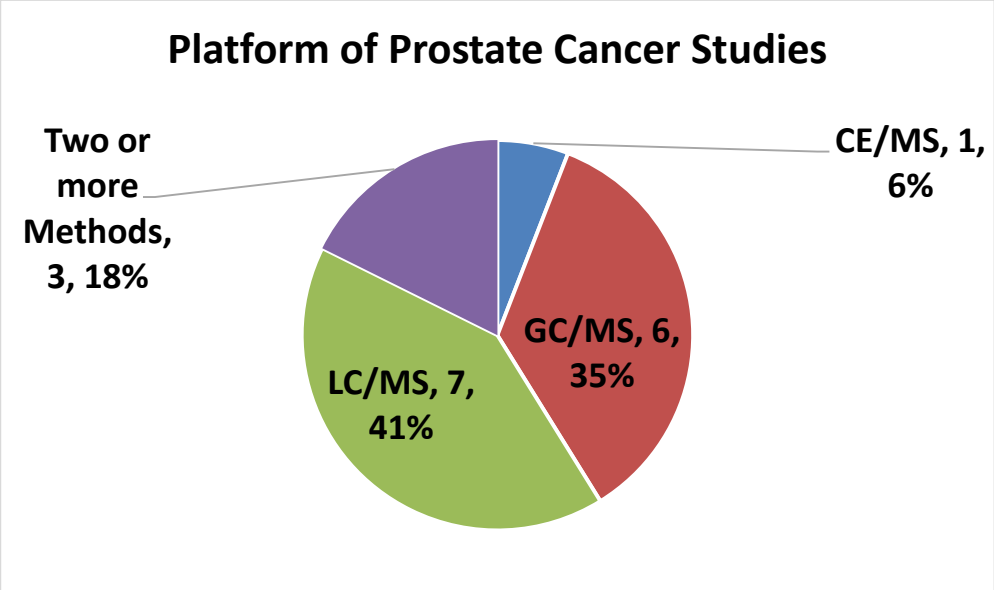

Figure 1.4 Pie diagram illustrating the types of analytical platforms used for prostate cancer studies. The number and percentage followed the name of the analytical platform represent the number of studies and the percentage in our study pool.

The highly polar metabolites analysis relies on more powerful techniques such as high-performance liquid chromatography (HPLC) and capillary electrophoresis (CE). The various chromatographic modes of HPLC such as ion exchange chromatography (IEC), normal phase (NP), reversed-phase (RP) and hydrophilic interaction liquid chromatography (HILIC) may employ MS compatible mobile phases. Thus, HPLC (7 studies. 41%) could provide good separation of different types of metabolites, give complementary understanding for metabolome and is the most popular separation platform for metabolome study to date. A high-resolution and more efficient form of HPLC is ultra-high pressure liquid chromatography (UPLC), which has superior speed and significantly higher sensitivity compared to conventional HPLC-MS. Several authors have reported a gold standard UPLC-MS because of the high peak capacity and low matrix effect. [25,36-38]

To profile different types of metabolites, nearly 18% studies used both LC/MS and GC/MS as hyphenated technologies for prostate cancer study. In an outstanding paper, Brown et al. used GC-MS and LC- MS to analyze methanolic extract in prostate and other biopsy samples. [16] In their study authors found 83 metabolites (out of a total of 260 different metabolites) to be promising markers. They connected these metabolites with cellular architecture and immunoreactivity by histopathological analysis. The 83 metabolites determined to be different between tumor containing sample and non-tumor containing sample among eight patients.

While only one paper is related to CE-MS in our study pool, it does not mean CE has less potential in prostate cancer metabolome. In a study reported by Kami and co-workers, concentration change of lactate, focusing on the phosphorylation analysis was found to be helpful in developing more effective bio-marker for anticancer therapy.[39] Considering the high selectivity, sensitivity and low sample demand for biological samples, CE-MS is a promising field to explore the potential of metabolites analysis.In addition, with the further advancement of sensitive detection and improvement of column technology more sensitive biomarker will be discovered by CE-MS.

1.4.4 Mass Spectrometer Types Used for Prostate Cancer

The most common mass analyzer used for metabolite identification is quadrupole time-of-flight (qTOF) (12%) and triple quadrupole (QqQ) (17%), as shown in Figure 1.5. Some paper also used Orbitrap alone or combined with quadrupole to get better results. Each MS analyzer has specific advantages and drawbacks. Therefore, it is important to use the most suitable MS which provides a balance among data quality (sensitivity, accuracy), time and cost consumption as well as research demanding (metabolic pathway, sample concentration, and stability). For example, if the research demanding is to quantitate the metabolites concentration level, QqQ should be the first choice

instead of TOF. Advantages and disadvantages of the aforementioned MS analyzers are discussed separately in the following paragraphs.

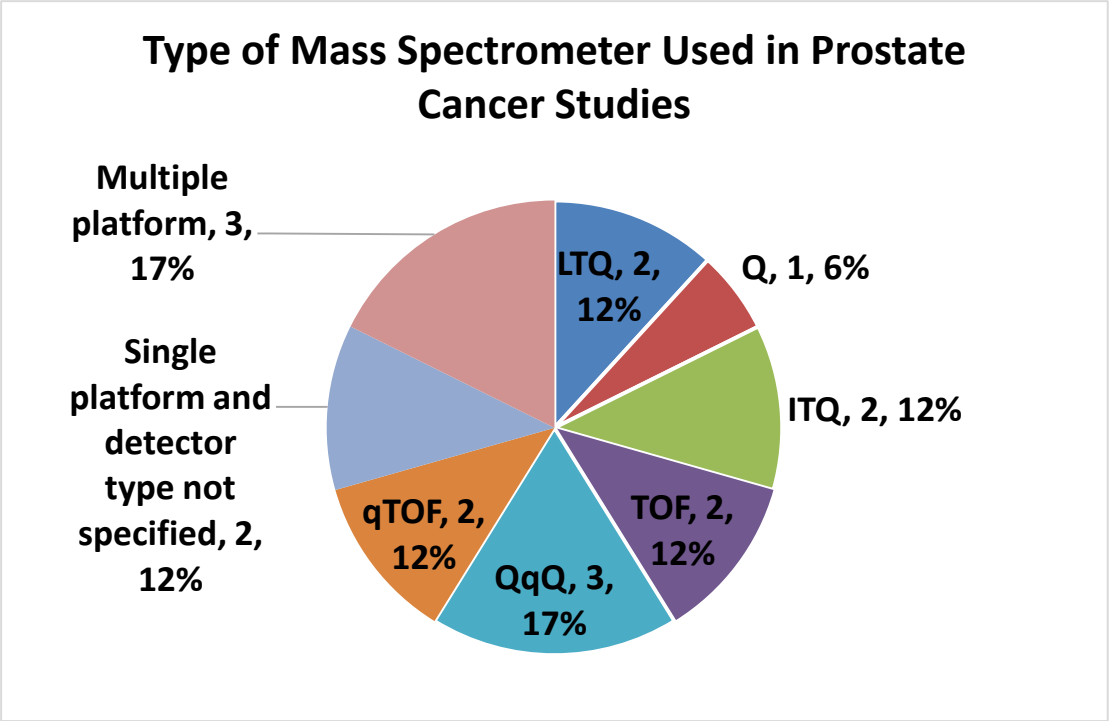

Figure 1.5 Pie diagram illustrating the types of mass spectrometer used for prostate cancer studies. The number and percentage followed the name of the mass spectrometer represent the number of studies and the percentage in our study pool.

As a traditional mass spectrometer in most analytical laboratories, QqQ is widely used in metabolites analysis. With excellent tandem MS capability, QqQ could provide information on structure determination of product ion, thereby reduce the possible structures, which could be applied in non-targeted metabolites profiling. Gaikwad successfully developed a method for more than 100 indigenous and exogenous steroid measurements in breast tissue in 12 minutes single UPLC-QqQ- MS/MS method. In this study, a simple liquid-liquid extraction was applied to extract 101 steroids followed by UPLC-MS/MS. The LOD for steroids metabolites is 0.001-15.7 pmol, suggesting the potential for clinical diagnosis for early stage prostate cancer. However, the linearity was not ideal with correlation coefficients (R^2) of only 0.90 for most of the analytes. [25]

Kapoore's group characterized eleven different classes' metabolites such as the pathway of amino acids, glucose, fatty acids and nucleotides with QqQ. A results showing difference of concentration level could aid the metabolomic interpretation and used for the therapy monitoring of prostate cancer.[40] With QqQ-MS detector, Liu's group[41] found the concentration level of one crucial steroidogenic enzyme, AKR1C3, is associated with the enzalutamide resistance and the targeting AKR1C3 could potentially increase the survival rate of prostate cancer patients.

However, due to the compromised duty cycle, quadruple MS loses partial sensitivity when a larger number of MS/MS data is acquired. To get more ion information, QqQ sacrifices either dwell time or data points collected on each peak. In contrast, qTOF allows analytes identification with accurate mass resolution and detection sensitivity in a rapid scan mode, without the need for prefiltration of certain predicted metabolites, which makes qTOF a cost and time effective mass analyzer, especially in the non-targeted metabolomic study. A study of the direct determination of small ribonucleic acids method was developed by Bartlett's group with ion exchange column. In their study, a set of RNAs in prostate cancer cells was identified with 6 ng/200,000 cells and LOQ of 6 ng/mL. With a one-step sample preparation, the recovery > 95% was obtained.[42] In the literature review, the qTOF is also most popular mass analyzer (65% in prostate cancer). Orbitrap was also discussed in some studies as part of tandem MS. McGinnis's group developed a method to quantitate the metabolites of siRNAs in a tissue sample with qTOF and applied the method for the determination of metabolism of and siRNA in prostate cancer.[42] Another application of qTOF is a study of Huang's group, in which a set of metabolites in cholesterol metabolic and mitogen-activated protein kinase signaling pathways were evaluated as a response to endocrine therapy to prostate cancer patients.[43] A similar prostate cancer therapy monitoring case was reported by Wei's

group, in which threonine, isoleucine, glutamine and linolenic acid pathway metabolites was studied with LC- QTOF-MS/MS.[44]

1.5 References

(1) Friedrich, C. G. *Advances in microbial physiology* **1997**, *39*, 235-289.
(2) Pace, N. R. *Proceedings of the National Academy of Sciences* **2001**, *98*, 805-808.
(3) Smith, E.; Morowitz, H. J. *Proceedings of the National Academy of Sciences of the United States of America* **2004**, *101*, 13168-13173.
(4) Ebenhöh, O.; Heinrich, R. *Bulletin of mathematical biology* **2001**, *63*, 21-55.
(5) Wishart, D. S.; Tzur, D.; Knox, C.; Eisner, R.; Guo, A. C.; Young, N.; Cheng, D.; Jewell, K.; Arndt, D.; Sawhney, S.; Fung, C.; Nikolai, L.; Lewis, M.; Coutouly, M. A.; Forsythe, I.; Tang, P.; Shrivastava, S.; Jeroncic, K.; Stothard, P.; Amegbey, G.; Block, D.; Hau, D. D.; Wagner, J.; Miniaci, J.; Clements, M.; Gebremedhin, M.; Guo, N.; Zhang, Y.; Duggan, G. E.; Macinnis, G. D.; Weljie, A. M.; Dowlatabadi, R.; Bamforth, F.; Clive, D.; Greiner, R.; Li, L.; Marrie, T.; Sykes, B. D.; Vogel, H. J.; Querengesser, L. *Nucleic acids research* **2007**, *35*, D521-526.
(6) Jewison, T.; Knox, C.; Neveu, V.; Djoumbou, Y.; Guo, A. C.; Lee, J.; Liu, P.; Mandal, R.; Krishnamurthy, R.; Sinelnikov, I.; Wilson, M.; Wishart, D. S. *Nucleic acids research* **2012**, *40*, D815-820.
(7) Nagrath, D.; Caneba, C.; Karedath, T.; Bellance, N. *Biochimica et Biophysica Acta (BBA)-Bioenergetics* **2011**, *1807*, 650-663.
(8) Mullen, A. R.; Wheaton, W. W.; Jin, E. S.; Chen, P.-H.; Sullivan, L. B.; Cheng, T.; Yang, Y.; Linehan, W. M.; Chandel, N. S.; DeBerardinis, R. J. *Nature* **2012**, *481*, 385-388.
(9) Idle, J. R.; Gonzalez, F. J. *Cell metabolism* **2007**, *6*, 348-351.
(10) Lanpher, B.; Brunetti-Pierri, N.; Lee, B. *Nature Reviews Genetics* **2006**, *7*, 449-459.
(11) Scriver, C. *Journal of inherited metabolic disease* **2001**, *24*, 093-116.
(12) Scriver, C. *Journal of inherited metabolic disease* **2004**, *27*, 305-317.
(13) Vangala, S.; Tonelli, A. *The AAPS journal* **2007**, *9*, E284-E297.
(14) Horgan, R. P.; Kenny, L. C. *The Obstetrician & Gynaecologist* **2011**, *13*, 189-195.
(15) Aboud, O. A.; Weiss, R. H. *Clinical chemistry* **2013**, *59*, 138-146.
(16) Brown, M. V.; McDunn, J. E.; Gunst, P. R.; Smith, E. M.; Milburn, M. V.; Troyer, D. A.; Lawton, K. A. *Genome Med* **2012**, *4*, 33.
(17) Gika, H. G.; Theodoridis, G. A.; Plumb, R. S.; Wilson, I. D. *Journal of Pharmaceutical and Biomedical Analysis* **2014**, *87*, 12-25.
(18) Aoki, W.; Tatsukami, Y.; Kitahara, N.; Matsui, K.; Morisaka, H.; Kuroda, K.; Ueda, M. *Journal of proteomics* **2013**, *91*, 417-429.
(19) Barbarin, N.; Mawhinney, D. B.; Black, R.; Henion, J. *J. Chromatogr. B: Anal. Technol. Biomed. Life Sci.* **2003**, *783*, 73-83.
(20) Cross, A. J.; Moore, S. C.; Boca, S.; Huang, W. Y.; Xiong, X.; Stolzenberg-Solomon, R.; Sinha, R.; Sampson, J. N. *Cancer* **2014**, *120*, 3049-3057.
(21) Davies, S. K.; Ang, J. E.; Revell, V. L.; Holmes, B.; Mann, A.; Robertson, F. P.; Cui, N.; Middleton, B.; Ackermann, K.; Kayser, M.; Thumser, A. E.; Raynaud, F. I.; Skene, D. J. *Proceedings of the National Academy of Sciences of the United States of America* **2014**, *111*, 10761-10766.
(22) Finkel, R. S.; Crawford, T. O.; Swoboda, K. J.; Kaufmann, P.; Juhasz, P.; Li, X.; Guo, Y.; Li, R. H.; Trachtenberg, F.; Forrest, S. J.; Kobayashi, D. T.; Chen, K. S.; Joyce, C. L.; Plasterer, T. *PloS one* **2012**, *7*, e35462.

(23) Aranibar, N.; Vassallo, J. D.; Rathmacher, J.; Stryker, S.; Zhang, Y.; Dai, J.; Janovitz, E. B.; Robertson, D.; Reily, M.; Lowe-Krentz, L.; Lehman-McKeeman, L. *Analytical biochemistry* **2011**, *410*, 84-91.
(24) Boda, D. *Curr. Proteomics* **2013**, *10*, 237-245.
(25) Gaikwad, N. W. *Anal. Chem. (Washington, DC, U. S.)* **2013**, *85*, 4951-4960.
(26) Gonzalez-Dominguez, R.; Garcia-Barrera, T.; Vitorica, J.; Gomez-Ariza, J. L. *Electrophoresis* **2015**, *36*, 577-587.
(27) Beger, R. *Metabolites* **2013**, *3*, 552.
(28) Crutchfield, C. A.; Olson, M. T.; Gourgari, E.; Nesterova, M.; Stratakis, C. A.; Yergey, A. L. *Journal of the American Society for Mass Spectrometry* **2013**, *24*, 230-237.
(29) Motsinger-Reif, A. A.; Zhu, H.; Kling, M. A.; Matson, W.; Sharma, S.; Fiehn, O.; Reif, D. M.; Appleby, D. H.; Doraiswamy, P. M.; Trojanowski, J. Q.; Kaddurah-Daouk, R.; Arnold, S. E. *Acta neuropathologica communications* **2013**, *1*, 28.
(30) Gonzalez-Dominguez, R.; Garcia-Barrera, T.; Gomez-Ariza, J. L. *J Pharm Biomed Anal* **2015**, *107*, 75-81.
(31) Sampson, J. N.; Boca, S. M.; Shu, X. O.; Stolzenberg-Solomon, R. Z.; Matthews, C. E.; Hsing, A. W.; Tan, Y. T.; Ji, B. T.; Chow, W. H.; Cai, Q.; Liu da, K.; Yang, G.; Xiang, Y. B.; Zheng, W.; Sinha, R.; Cross, A. J.; Moore, S. C. *Cancer Epidemiol Biomarkers Prev* **2013**, *22*, 631-640.
(32) Wuolikainen, A.; Moritz, T.; Marklund, S. L.; Antti, H.; Andersen, P. M. *PloS one* **2011**, *6*, e17947.
(33) Figueroa, J. D.; Cordero, K.; Serrano-Illan, M.; Almeyda, A.; Baldeosingh, K.; Almaguel, F. G.; De Leon, M. *Neuroscience* **2013**, *255*, 1-18.
(34) Kuhara, T.; Ohse, M.; Inoue, Y.; Shinka, T. *Journal of Mass Spectrometry* **2009**, *44*, 214-221.
(35) Wu, H.; Liu, T.; Ma, C.; Xue, R.; Deng, C.; Zeng, H.; Shen, X. *Anal. Bioanal. Chem.* **2011**, *401*, 635-646.
(36) Andreas, N. J.; Hyde, M. J.; Gomez-Romero, M.; Angeles Lopez-Gonzalvez, M.; Villasenor, A.; Wijeyesekera, A.; Barbas, C.; Modi, N.; Holmes, E.; Garcia-Perez, I. *Electrophoresis* **2015**, *36*, 2269-2285.
(37) Cai, Y.; Liu, Y.; Helmy, R.; Chen, H. *J. Am. Soc. Mass Spectrom.* **2014**, *25*, 1820-1823.
(38) WO2014089431A1, 2014.
(39) Kami, K.; Fujimori, T.; Sato, H.; Sato, M.; Yamamoto, H.; Ohashi, Y.; Sugiyama, N.; Ishihama, Y.; Onozuka, H.; Ochiai, A.; Esumi, H.; Soga, T.; Tomita, M. *Metabolomics : Official journal of the Metabolomic Society* **2013**, *9*, 444-453.
(40) Kapoore, R. V.; Coyle, R.; Staton, C. A.; Brown, N. J.; Vaidyanathan, S. *Metabolomics : Official journal of the Metabolomic Society* **2015**, *11*, 1743-1755.
(41) Liu, C.; Lou, W.; Zhu, Y.; Yang, J. C.; Nadiminty, N.; Gaikwad, N. W.; Evans, C. P.; Gao, A. C. *Cancer research* **2015**, *75*, 1413-1422.
(42) McGinnis, A. C.; Cummings, B. S.; Bartlett, M. G. *Anal Chim Acta* **2013**, *799*, 57-67.
(43) Huang, G.; Liu, X.; Jiao, L.; Xu, C.; Zhang, Z.; Wang, L.; Li, Y.; Yang, C.; Zhang, W.; Sun, Y. *Eur. J. Pharmacol.* **2014**, *729*, 132-137.
(44) Wei, C.; Li, Y.; Yao, H.; Liu, H.; Zhang, X.; Guo, R. *Molecular bioSystems* **2012**, *8*, 2197-2204.

(45) Brown, M. V.; McDunn, J. E.; Gunst, P. R.; Smith, E. M.; Milburn, M. V.; Troyer, D. A.; Lawton, K. A. *Genome Med.* **2012**, *4*, 33.
(46) Hu, Y.; Qi, Y.; Liu, H.; Fan, G.; Chai, Y. *Biochimica Et Biophysica Acta-General Subjects* **2013**, *1830*, 2779-2789.
(47) Brockmoeller, S. F.; Bucher, E.; Mueller, B. M.; Budczies, J.; Hilvo, M.; Griffin, J. L.; Oresic, M.; Kallioniemi, O.; Iljin, K.; Loibl, S.; Darb-Esfahani, S.; Sinn, B. V.; Klauschen, F.; Prinzler, J.; Bangemann, N.; Ismaeel, F.; Fiehn, O.; Dietel, M.; Denkert, C. *Journal of proteome research* **2012**, *11*, 850-860.
(48) Troyer, D. A.; Shuster, J. R.; Lance, R. *Modern Pathology* **2013**, *26*, 502A-502A.
(49) Nacoulma, A. P.; Vandeputte, O. M.; De Lorenzi, M.; El Jaziri, M.; Duez, P. *Int. J. Mol. Sci.* **2013**, *14*, 12533-12549, 12517 pp.
(50) Wei, S.; Liu, L.; Zhang, J.; Bowers, J.; Gowda, G. A. N.; Seeger, H.; Fehm, T.; Neubauer, H. J.; Vogel, U.; Clare, S. E.; Raftery, D. *Molecular Oncology* **2013**, *7*, 297-307.
(51) Li, C.; Zang, T.; Wrobel, K.; Huang, J. T. J.; Nabi, G. *Anal. Bioanal. Chem.* **2015**, *407*, 3393-3404.
(52) Guertin, K. A.; Loftfield, E.; Boca, S. M.; Sampson, J. N.; Moore, S. C.; Xiao, Q.; Huang, W. Y.; Xiong, X.; Freedman, N. D.; Cross, A. J.; Sinha, R. *The American journal of clinical nutrition* **2015**, *101*, 1000-1011.
(53) Struck-Lewicka, W.; Kordalewska, M.; Bujak, R.; Mpanga, A. Y.; Markuszewski, M.; Jacyna, J.; Matuszewski, M.; Kaliszan, R.; Markuszewski, M. J. *Journal of Pharmaceutical and Biomedical Analysis* **2015**, *111*, 351-361.

CHAPTER 2: Method Development and Quantitation of Metabolites in Prostate Tissue Samples by Capillary Electochromatography-Mass Spectrometry

2.1 Abstract

Prostate cancer is the second "killer"cancer among males worldwide. However, there are only few reports for early diagnosis s of prostate cancer. The aim of this project was to develop a quantitative capillary electrochromatography coupled to tandem mass spectrometry (CEC-MS/MS) for metabolic profiling in prostate needle biopsy extracts, based on extraction and fixation (mPREF) technique developed by Troyer's and coworkers.[1] Through a one-step in situ polymerization, a modified polymer monolith was successfully synthesized and characterize. With vinylbenzyl trimethylammonium chloride (VBTA) as a monomer and a hybrid crosslinker bisphenol a glycerolate dimethacrylate (BisGMA) and ethylene glycol dimethacrylate (EDMA), this column has strong separation selectivity for hydrophilic metabolites. The effect of mobile phase pH, ACN percentage and volatile additive were optimized. The CEC-MS/MS was found to be highly robust with limit of detection (LOD) for the metabolites to range between 50 -100 nM. The validated CEC-MS/MS method was able to differentiate and quantitate between normal versus tumor tissue in 22 human subjects. This method could be s successfully used to examine prostate cancer with an accuracy of 95%.

2.2 Introduction

One of the most common malignant tumors, prostate cancer[1-3] is heterogeneous in clinical settings and has a highly variable natural history. For prostate cancer diagnosis and prognosis, the present methods have limitations making quantitative information to be valuable for patients and physicians. Currently, there is a need to generate new quantitative method to assist in the diagnosis

and prognosis of prostate cancer by clinicians and pathologists. Troyer's and coworkers used molecular preservation by extraction and fixation ("mPREF"), which includes a procedure to extract small molecules by liquid-liquid extraction using aqueous methanolic solvent.[1] One of the main advantages of mPREF is the ease with which conventional histology can be performed on the same tissue. This unique feature of mPREF enables quantitation of small molecule metabolites. With this method, one can screen for prostate cancer to provide the biopsy sample with useful information on metabolites concentration change in the cancer-containing and non-cancer containing tissue samples. In a proof-of-principle studies, Troyer's and coworkers identified eight significant metabolites [uracil, alanine, proline, malate, xanthine, betaine, *N*-acetyl aspartic acid (NAA) and *N*-acetyl-glucosamine (NAG) with concentration level difference between tumor and non-tumor samples. Currently there exists a need for analytical methods that permit the separation and quantitation of aforementioned polar metabolites. Procedures utilizing gas chromatography (GC)[4] or liquid chromatography (LC) [5,6] have been developed, but are restricted to the analysis limited biomarkers for detection of prostate cancer. In addition, for most of metabolites, the available LC or GC column could not meet the demand of separation selectivity. Most of the published HPLC methods are time consuming require expensive columns and employ gradient elution or multi-step separation and detection.

Capillary electrochromatography (CEC)[7] is a hybrid of HPLC and CE with the combination of advantages for both HPLC and CE techniques. In recent years, CEC has attracted more and more attention because of the benefits of low injection size in volume limited biological samples. Due to the flexibility of stationary phase, fritless design and excellent performance, the polymer monolith is one of the most suitable format in CEC. However, the low sample capacity in CEC and trace level analysis of small molecules in biological samples requires a high sensitivity

detector based on mass spectrometry (MS). The most popular ionization source for CEC is the use of electrospray Ionization (ESI). With the help of sheath liquid and ESI source[8], the ionic or polar compounds separated by the CEC under low flow conditions (low nL/min range) can be efficiently transferred from the liquid phase into gas phase ions required by MS instruments. In addition, ESI-MS relies on the production of ions which are multiply charged. The newly emerging hyphenated technique such as CEC-MS distinguishes analytes by both their differences in electrophoretic mobilities and stationary phase retention whereas MS could detect the eluted compounds based on differences in mass-to-charge-ratio. Thus, CEC-MS combines the advantages of both CEC and MS providing high separation efficiency, determining molecular masses and/or structural information in one analysis.

As mentioned earlier, previous research by Troyer et al. identified a subset of metabolites from prostate needle biopsy prepared using the mPREF method as potential prostate cancer diagnostic markers. These markers were stratified based on the analytical technique mostly applicable for metabolite quantitation to be used in future verification studies and possible diagnostic assay development. In this work, a CEC-MS assay is develop to quantitate eight proof of concept (POC) metabolites that are selected from the candidate list[1] including betaine, malate, proline, NAA, NAG, uracil, xanthine, and alanine in human tissue biopsy extracts. The structure of metabolites is shown in Figure 2.1.

2.3 Experimental Section

2.3.1 Chemicals and Reagents

Vinylbenzyl trimethylammonium chloride (VBTA), Bisphenol A glycerolate dimeth-acrylate (BisGMA), 2, 2′- azobis (2-methylpropionitrile) (AIBN), 3-(trimethoxy-silyl)propyl methacrylate (γ-MAPS) were purchased from Sigma-Aldrich (St. Louis, MO). Ethylene glycol dimethacrylate (EDMA) purchased from Sigma-Aldrich was distilled to remove inhibitor before its usage. The HPLC grade acetonitrile (ACN), methanol (MeOH), triethylamine (TEA), butylamine (BA), valeric acid (VA), heptaflurobutyric acid (HFBA), and 7.5 M ammonium acetate (NH_4OAc) aqueous solution, dimethyl sulfoxide (DMSO), alanine, uracil, malate, proline, NAA, NAG, betaine and xanthine were all obtained from Sigma-Aldrich (St. Louis, MO). All isotope labeled chemicals for the quantitation were obtained as follows, [D-alanine-2-d1, uracil-5-d1, N-(carboxymethyl)-N,N,N-trimethyl-d3-ammonium Chloride (N-methyl-d3), D-proline-2,5,5-d3 from CDN Isotopes]; malic acid- L-[14C(U)] and *N*-acetyl aspartic acid, DL-[2,3-3H] from ARC; xanthine- 13C-15N2 from Alsachim; *N*-acetyl-D-[1-13C] glucosamine from Omicron. Triply deionized water (TDI, 18.2 MΩcm) was generated in the laboratory using Barnstead Nanopure II Water System (Dubuque, IA). All the chemicals have above 98% purity.

2.3.2 Preparation of Monolithic Columns

Two different pretreatment procedures could be use to prepare the monolithic column. For the first procedure, a 60 cm long fused silica capillary (360 μm o.d., 100 μm i.d., Polymicro Technologies, Phoenix, AZ) was flushed under vacuum with acetone and 1 M NaOH for 15 min each. Next, the capillary was filled with 1 M NaOH and both ends were sealed with rubber septa and heated at 100 °C for 2 h in a GC oven Finally, the capillary was flushed with triply deionized water, 1 M

HCl, triply deionized H_2O, and MeOH for 15 min each under vacuum. A solution of γ-MAPS (50%, v/v in anhydrous MeOH) was then filled through the capillary under vacuum. The filled capillary was once again sealed with rubber septa and kept at 50 °C for 14 h in a GC oven.

The second procedure also started with 60 cm long fused silica capillary (360 μm o.d., 100 μm i.d.). The capillary is flushed under vacuum with 1 M NaOH solution, triply deionized water, 0.1 M HCl, triply deionized water and MeOH for 3, 0.5, 0.5, 0.5 and 0.5 hrs, respectively. Next, the capillary is flushed under vacuum with HPLC grade anhydrous MeOH for 0.5 hrs. Finally, the capillary is flushed under vacuum with γ-MAPS (50%, v/v in anhydrous MeOH) for ~ 0.5hrs. The filled capillary sealed with rubber septa is then placed at 60 ˚C for 20 h in a GC oven.

Both procedures were tested, and there were not much difference on the column performance. Most experiments in this study followed the second procedure.

Next, the unreacted γ-MAPS solution was removed by flushing the capillary under vacuum using acetone for 5 min. The vinylized capillary was eventually dried under nitrogen for 3 h at 60 °C in a GC oven.

A typical procedure for making monolithic columns is shown in Scheme 1 and described as follows. First, 10mg (10%, w/w) of the VBTA and 1 mg of AIBN were dissolved in a mixture containing various compositions of crosslinker (% w/w) of BisGMA and EDMA, Table 2.1).

Table 2.1 Effect of binary crosslinker composition on physical characteristics of monolithic columns.

*Column	Crosslinker: EDMA (wt%)	Crosslinker: BisGMA (wt%)	Porosity ε_T	Permeability ($\times 10^{-15} m^{2)}$ K_o	EOF ($cm^2v^{-1}s^{-1}$)

A	20	0	0.81	3.63	6.43E-04
B	15	5	0.74	2.68	6.19E-04
C	10	10	0.70	2.38	2.97E-04
D	5	15	0.65	2.26	1.78E-04
E	0	20	0.93	5.25	3.23E-04

* All columns A-E were polymerized using 10% (wt/wt) VBTA as functional monomer , 19% (wt/wt) methanol and 51% (wt/wt) of dodecanol as porogens , AIBN 1%. (wt/wt) as initiator

To each of the mixture, porogens (dodecanol and MeOH) was added. The final polymerization solution was then ultrasonicated for 30 min before filling the solution to the pretreated capillary with a handheld syringe. Typically, in the preparation of CEC-MS column, 30 cm out of 60 cm of the pretreated capillary was filled. The column was then sealed with rubber septa and was kept at 60 °C in a GC oven to polymerize. After 20 h of polymerization, the column was flushed with ACN for 24 h to remove the unreacted monomers. The monolithic capillary was conditioned for 24 h with mobile phase before use.

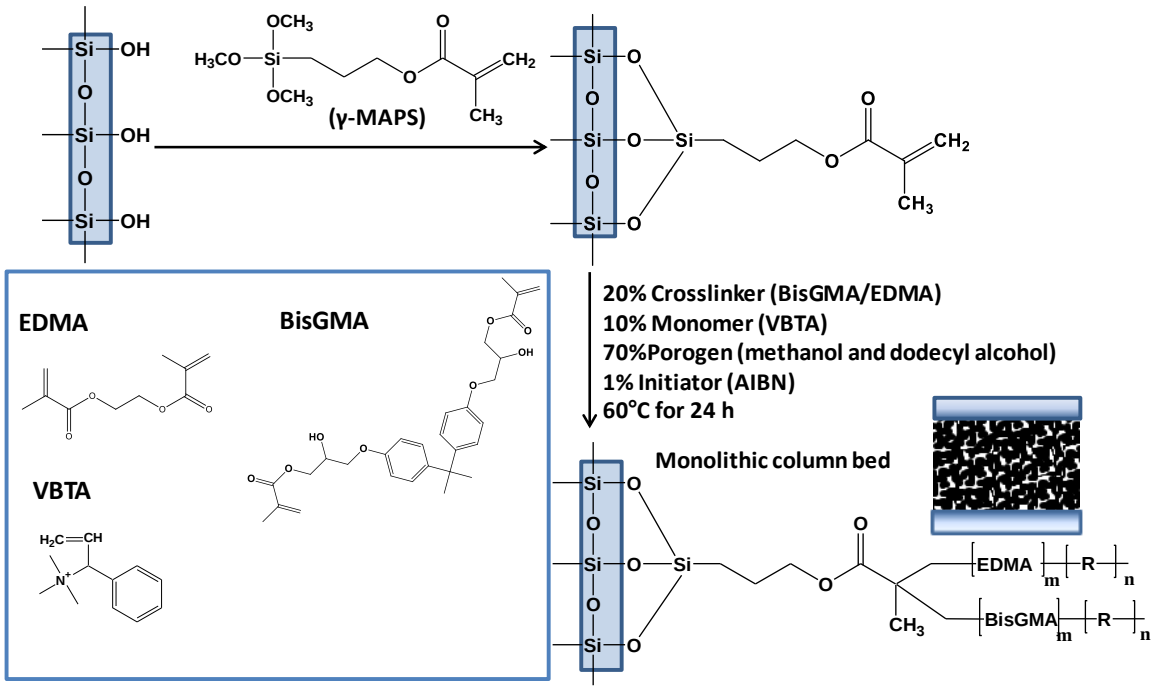

Scheme 1. Synthetic scheme for the preparation of poly (VBTA-co-BisGMA/EDMA) monolithic column. The chemical structures of monomer and crosslinkers are shown in the inset box to the left. R stands for the monomer VBTA. The letter m and n is the degree of polymerization.

2.3.3 Morphology Measurements

A Hitachi X-650 (Hitachi, Japan) scanning electron microscope (SEM), which is part of Georgia State University core facility, was used to characterize the microscopic morphology of the monolithic columns. Monolithic columns samples were cut to 2 mm in length and placed on an aluminum stub by double-sided carbon tape. The samples were then sputter-coated with gold/palladium alloy with a SPI sputter.

2.3.4 CEC-MS/MS Instrumentation

All CE experiments were performed on Agilent G7100 CE system (Agilent Technologies, Palo Alto, CA). Agilent QqQ MS/MS was used as a detector to collect all MS data was equipped with Agilent CE-MS adapter kit (G1603A), an Agilent CE-ESI-MS sprayer kit (G1607) and Agilent

1100 series isocratic HPLC pump to deliver the sheath liquid with a 1:100 splitter. Nitrogen was used both as a nebulizing gas and drying gas. An Agilent 1100 LC equipped with MS/MS was used to optimize the MRM parameters of all analytes. A series III isocratic HPLC pump (Lab Alliance, State College, PA) was used to flush and condition the column. An Ultra-Plus II micro-HPLC system (Micro-Tech Scientific Inc., Fontana, CA) was used for the measurement of porosity and permeability.

2.3.5 Monolithic Column Conditioning

After 20 h of polymerization, the column was flushed with ACN for 24 h to remove the unreacted monomers. The monolithic capillary was conditioned for 24 h with mobile phase before use. Before a monolithic column was installed in CE-MScartridge, the monolithic column was equilibrated with by stepwise voltage conditioning from 2-15 kV using CE-UV cartridge in which both ends were immersed in mobile phase. At the completion of voltage conditioning, the monolithic column is quickly transferred from CE-UV to CE-MS cartridge and inserted in the CE nebulizer. Before installation of the capillary in the nebulizer, care is taken to ensure that the inlet lift of the CE instrument is in the upright position.

2.3.6 Buffer and Analyte Preparation

Various parameters were used to optimize the CEC-MS conditions to get best separation and detection as following: A series of BGEs containing 15 mM NH_4OAc were studied over an extensive pH range from 2.5 to 11.0 in 1.0 unit increment. Because the natural (unadjusted) pH of 15 mM NH4OAC is 6.8), for pH lower and higher than the unadjusted pH value, 1 M acetic acid and 1 M ammonium hydroxide was used to obtain the desired pH of the BGE. The unadjusted pH of BGEs containing HFBA, BA, TEA and VA were 1.7, 10.0, 11.0 and 3.3, respectively. Acetic

acid and ammonium hydroxide were used to adjust the pH to 1.8. The mobile phases, which contains a mixture of 50% – 90% (v/v) ACN, 15 mM HFBA at pH 1.8 were prepared as follows. Aliquots of 0.195mL of HFBA and 0.133 mL of 7.5M NH_4OAc were mixed with a certain percentage of ACN and water in a 100 mL centrifuge tube. The aqueous-organic mixture is then vortex, sonicated and degassed. Stock solutions of each standard POC metabolite standards were prepared at 50 mM by dissolving in TDI. Working analyte solutions were prepared at 500 μM by diluting the analyte stock solution into 50/50 ACN/H_2O (v/v). Injections were performed electrokinetically at +5 kV for 10 sec. Analytes strcture and predicted propertity is shown in Figure 2.1.

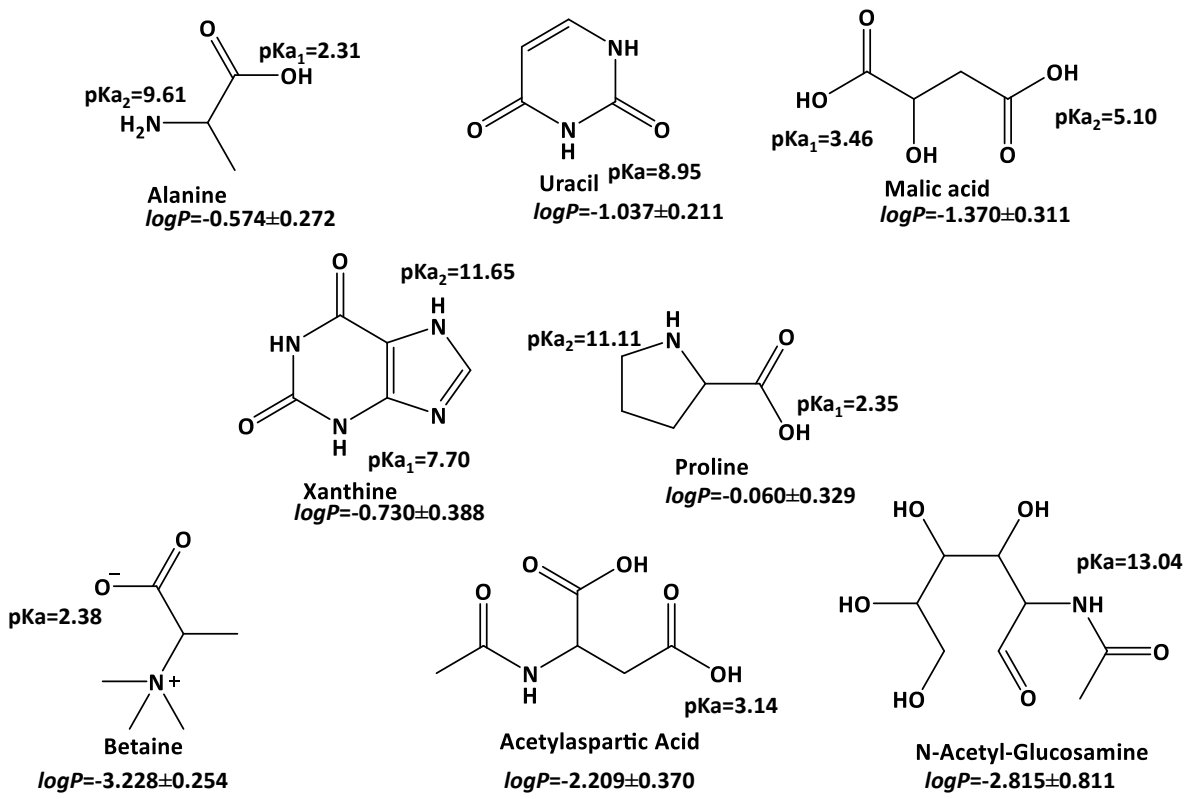

Figure 2.1 Chemical structures of all POC metabolites.

2.3.7 Calculations

The chromatographic retention factor was calculated using the following equation:

$$k' = \frac{t_R - t_m}{t_m} \qquad (1)$$

where k' is the retention factor for neutral compounds, t_R and t_m are the retention times of the analyte and the dead time marker (DMSO), respectively.

For ionic compounds, a modified equation was used

$$k^* = \frac{k' - \mu_{ep} / \mu_{eo}}{1 + \mu_{ep} / \mu_{eo}} \quad (2)$$

In equation (2) k^* is the electrochromatographic retention factor, μ_{ep} is the electrophoretic mobility of the charged solute and μ_{eo} is the electroosmotic mobility. μ_{ep} and μ_{eo} were obtained from open tubular column.

The porosity of the CEC monolithic columns was calculated by the following method. The porosity experiment was carried out on a micro-HPLC system, in which the volumetric flow rate V (m^3/s) was measured by weighing the mobile phase (pure ACN) flowing through the column in a certain amount of time. The linear velocity of the mobile phase u (m/s) was measured by taking a ratio of column length with an untrained dead time marker. The porosity was calculated by the following equation:

$$\varepsilon_T = \frac{V}{\pi r^2 u} \times 100\% \qquad (3)$$

Where ε_T is the total porosity of the column; r (m) is the inner radius of the column.

The specific permeability of the monolithic column was calculated by:

$$K^0 = \frac{u \eta L \varepsilon_T}{\Delta p} \qquad (4)$$

where η (Pa s) is the dynamic viscosity of the mobile phase; L (m) is the effective length of the column; Δp (Pa) is the pressure drop along the column.

2.4 Results and Discussion

2.4.1 Characterization of monolithic columns

VBTA is positively charged compound with quaternary ammonium and a vinylbenzyl group, which was widely used as a monomer in monolith to provide ion interaction and π- π interaction with analytes. [9-11] Lin's[10] group has synthesized a monolithic column with VBTA as a monomer and hydrophilic BisGMA as a crosslinker and successfully applied into the separation of polar analytes such as uracil, uridine, adenine, etc. in CEC with UV detection. To achieve simultaneous separation of the targeted metabolites in the biopsy extracts, the percentage of binary crosslinker (EDMA and BisGMA) were carefully optimized the get the best monolith stationary phase compatible for CEC-MS/MS. Five possible recipes of polymerization mixture with the various ratio (% w/w) of EDMA and BisGMA) were used to make monolithic columns as shown in Table 2.1. The data listed in Table 2.1 suggest that binary mixture of crosslinkers of EDMA-BisGMA provide lower porosity (ε_T) and permeability (Ko) compared to the use of single crosslinker. The

column permeability follows the order: column E >column A> column B> column C. >column D. Thus, BisGMA is more permeable than EDMA as a single crosslinker, but increasing the ratio of BisGMA decreases the porosity and permeability as well as electroosmotic flow (EOF).The SEM photographs of the five monolithic CEC columns under the optimum polymerization conditions are shown in Figure 2.2. From the SEM micrographs, one can observe that the spherical units are agglomerated into clusters in column A-D, and monolith was successfully formed in the CEC capillary with through pores evenly distributed and homogeneous. By comparing A1 and D1, the through-pore size decreased along with the increase in BisGMA from around 5μm to 1μm. For column A-D the through pore size decreases as shown in the SEM pictures of each column. A conclusion could be made that along with the through-pore size decrease and polymer cluster size decrease, the open space in the monolith become less and more difficult for fluid (ACN) to move through the column.

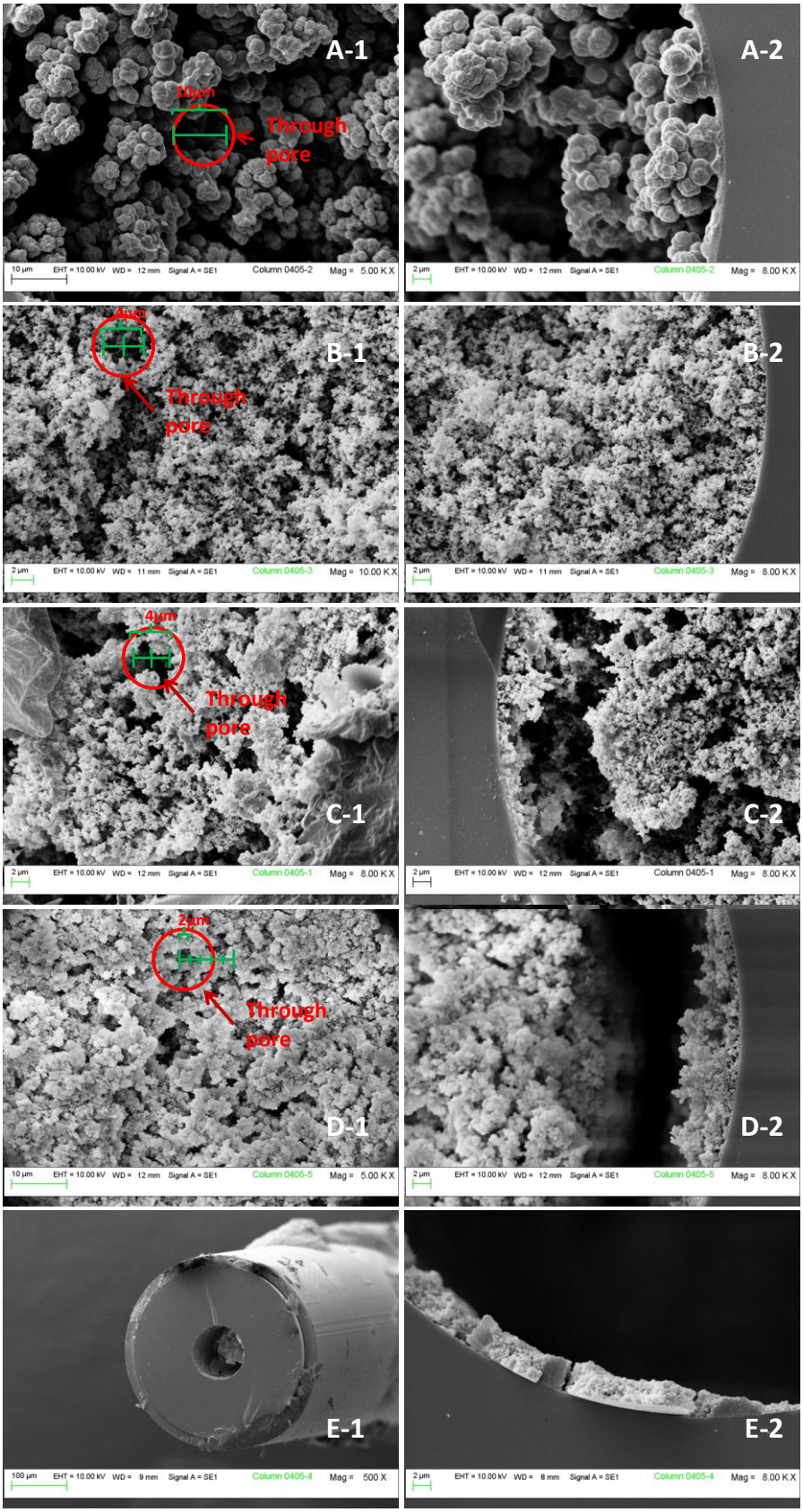
A-1
10μm
Through pore
A-2
B-1
4μm
Through pore
B-2
C-1
4μm
Through pore
C-2
D-1
2μm
Through pore
D-2
E-1
E-2

Figure 2.2 Scanning electron micrographs (SEMs) of monolith columns with different crosslinker ratio. A: EDMA:BisGMA 20:0; B: EDMA:BisGMA 15:5; C: EDMA:BisGMA 10:10; D: EDMA:BisGMA 5:15; E: EDMA:BisGMA 0:20. Detailed information of the polymerization mixture composition for the monolith is described in Table 2.1. A-1 and A-2 represents the SEM picture s of polymer monolith and the edge section of polymer and the capillary inner wall of column A, respectively. The SEM scale bar was measured as follows: A-1 (10μm), A-2 (2μm), B-1 (2μm), B-2 (2μm), C-1 (2μm), C-2 (2μm), D-1 (10μm), D-2 (2μm), E-1 (100μm), E-2 (2μm).

At 10:10 BisGMA: EDMA ratio (Figure 2.2C) a gap between the monolith and capillary inner wall appeared and was progressively worse with the increase in BisGMA content (Figure 2.2 E). When the column E was flushed with ACN to get rid of unreacted porogens, a piece of white solid clump was observed to fall off. In particular, Figure 2.2 E-2, shows a significant gap inside the capillary column, due to swelling of monolith. For the column E, the sudden high porosity and permeability in Table 2.1 is related to hollow morphology inside the column, which is more like a thin layer coated column instead of real monolith formation.

The overlaid plots of the back pressure vs. the volumetric flow rate observed on the five monolithic columns are shown in Figure 2.3. Consistent with the lowest values of porosity ε_T and permeability K_o in Table 2.1, the column D with a ratio of 5:15 for EDMA-BisGMA provided the highest back pressure, i.e., the slope of pressure vs. flow rate is the steepest. On the other hand, column E with only BisGMA as a crosslinker has significantly lower back pressure, consequently much shallower slope. Nevertheless, it is obvious that the linearity of back pressure to flow rate for all five plots is very good, which means the mechanical stability of monolithic column A-D monolithic columns is excellent under the pressure of even 25 Mpa.

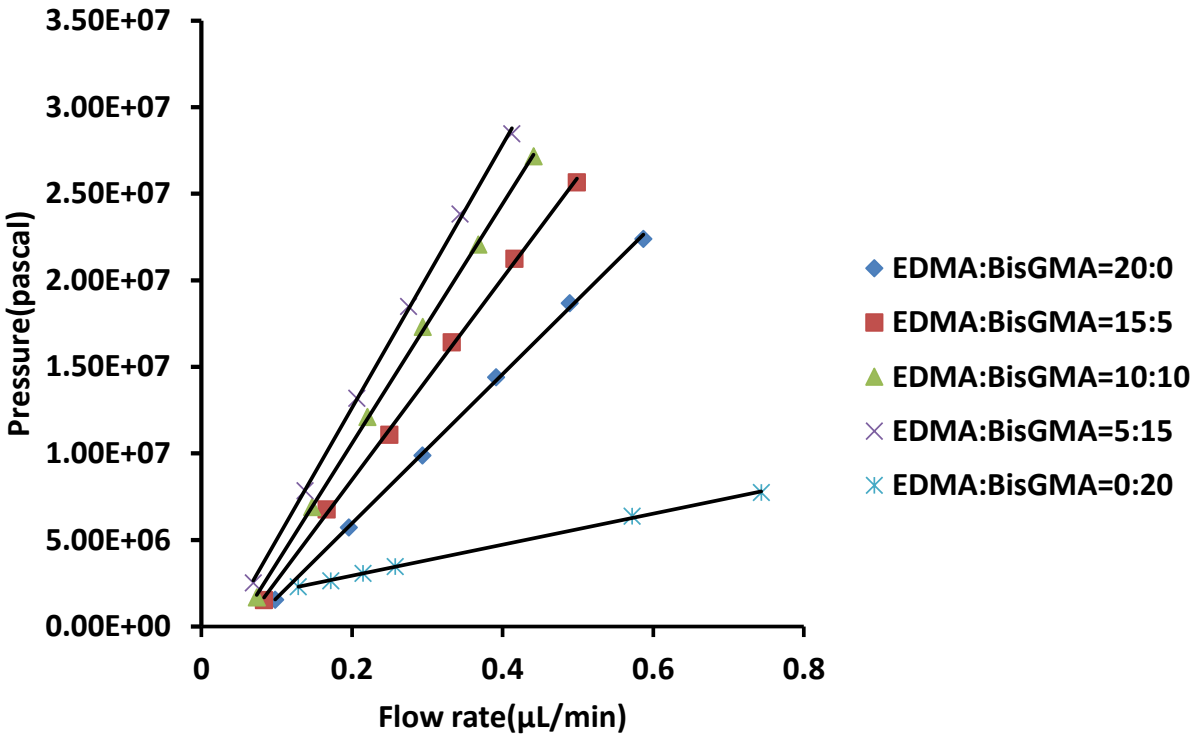

Figure 2.3 Plots of the applied pressure against the volumetric flow rate of ACN in the micro-HPLC experiment. Mobile phase: pure ACN. The composition of each columns are described in Table 2.1.

From the evidence on column characterization, column C-E was eliminated from the list due to the inhomogeneous polymer monolith. Column A was also not under consideration because the BisGMA percentage is 0 and lack of hydrophilic group on the monolith important for the separation selectivity of POC polar metabolites. More data will be presented in the following section to support this decision.

2.4.2 Mobile Phase Optimization

2.4.2.1 Effect of Mobile Phase pH

A series of BGEs containing 15 mM NH_4OAc were studied over a pH range from 2.5 to 11.0 in 1.0 unit increment, as shown in Figure 2.4. At pH lower than 2.0, the silanol groups on the surface of column are protonated. At pH 2.5-6.0, metabolites alanine, proline, and NAG are neutral, while xanthine and uracil positive are changed and malic acid negative charged, showing a flat profile, except for betaine which exists as a zwitterionic compound at pH five due to ionization of carboxylate group, which perhaps interacts with positive charges on the VBTA monolith. Interestingly, between pH 7-8, separation factor drops for all metabolites due to increasing in t_0 value (Figure 2.4). Another drop was seen for all analytes between pH 10-11 for the same reason of decreased t_0 value.

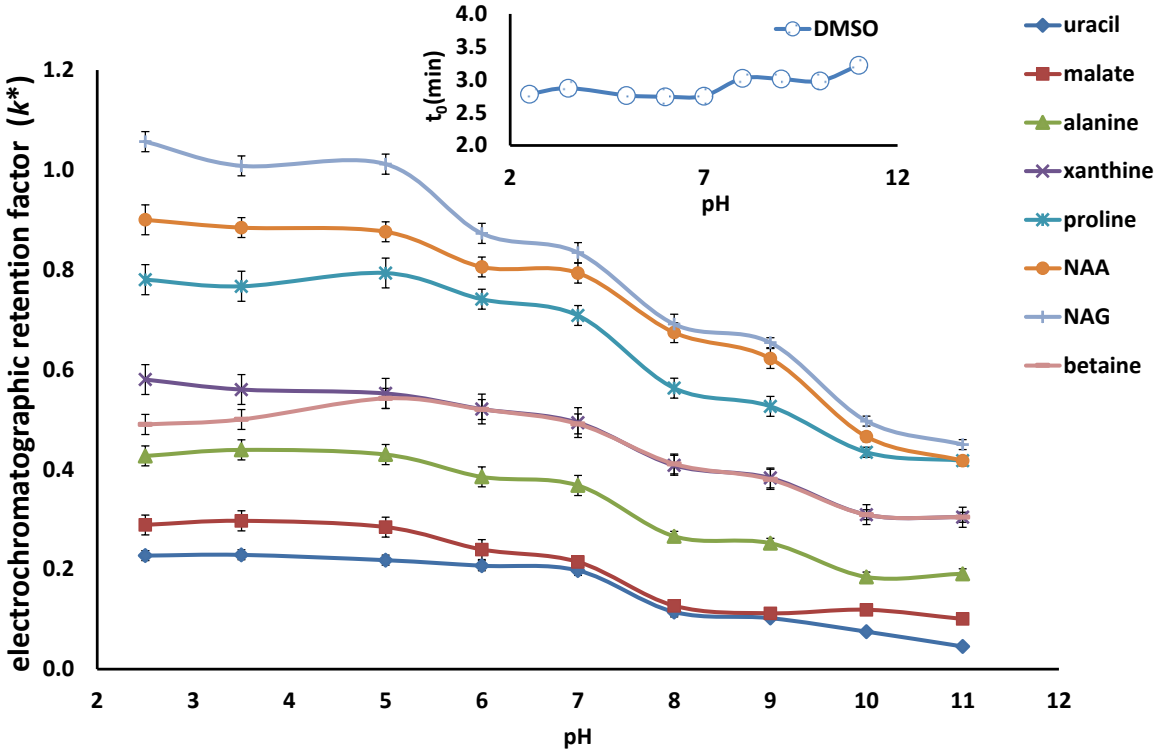

Figure 2.4 Effect of the buffer pH values on the retention factors of eight POC metabolites. Conditions: CEC-ESI-MS/MS using monolith poly (VBTA-co-BisGMA/EDMA). The experiment was performed on 60 cm(100 μm I.D.). Running buffer: 75/25 ACN/water, 15mM NH_4OAc, pH varies; Voltage: +15 kV; Capillary temperature, 20 °C. Injection: 5 mbar, 100 s; MS conditions: sheath liquid, MeOH/H_2O (80/20, v/v) containing 40 mM HOAc; sheath liquid flow rate, 5 μL/min; capillary voltage, +3500V; drying gas flow rate, 5.0 L/min; drying gas temperature, 200 ◦C; nebulizer pressure, 7 psi.

When pH is lower than 2.5, a large amount of acetic acid was added to adjust the pH and the monolithic bed start deteriorating after around 20 runs due to the high salt concentration in the buffer. Therefore, another BGE such as HFBA was introduced in the lower pH range because of its lower *pKa* and compatibility to MS. The separation of metabolites are shown using HFBA at three different pH values are shown in Figure 2.5. Clearly, a decrease in mobile phase pH from 2.5 to 1.8 increases the resolution between two peak pairs (betaine/xanthine) and

(proline/acetylaspartic acid) to 1.45 and 2.30, respectively. As a result, pH 1.8 was chosen as the optimum pH for the CEC-MS of POC metabolites.

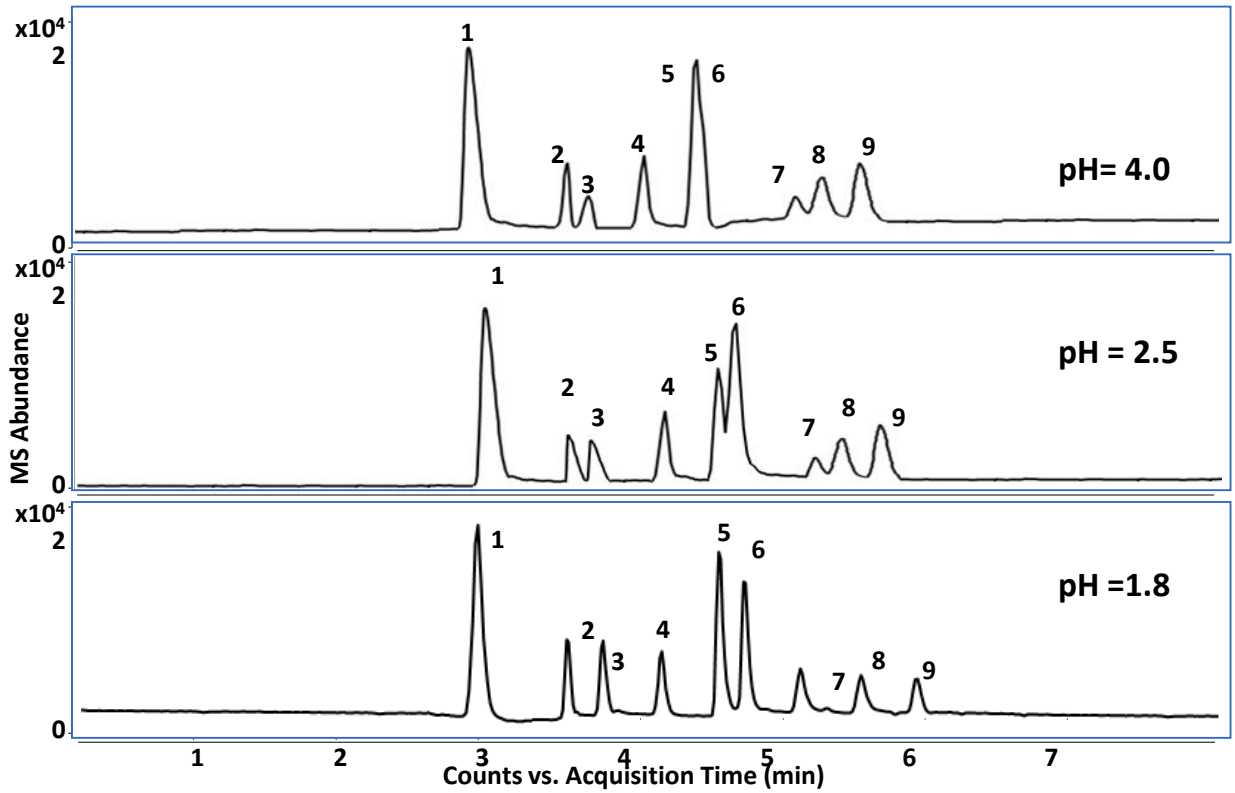

Figure 2.5 Effect of mobile phase pH on simultaneous separation of eight proof of concept (POC) metabolites. Conditions: CEC-ESI-MS/MS using monolith poly (VBTA-co-BisGMA/EDMA). Experiment was performed on 60 cm(100 μm I.D.). Running buffer: 75/25 ACN/water, 15mM heptflurobutyric acid, (a). pH= 4.0, (5). pH= 2.5, (c). pH= 1.8, Voltage: +15 kV; ; Capillary temperature, 20 °C. Injection: 5 kV 10s; ESI-MS conditions are the same as Figure 3. Peak identification: (1) dimethylsulfoxide; (2) uracil; (3) malate; (4) alanine; (5) betaine; (6) xanthine; (7) proline; (8) acetylaspartic acid; (9) acetylglucosamine.

2.4.2.2 Effect of Acetonitrile

The percentage of ACN was varied from 50% (v/v) ACN to 90% (v/v) ACN to optimize the run time and separation of POC metabolites. The *k** of metabolites was calculated based on different ACN percentage in the buffer. In Figure 2.6, the *k** of all compounds increase nearly two folds with the increase of ACN. A conclusion could be drawn that hydrophilic interaction seems to be

the primary mechanism of interaction between solutes and the monolithic column. The use of 75% (v/v) of ACN was chosen as the optimum organic solvent percentage due to a good compromise between analysis time and resolution of the metabolites.

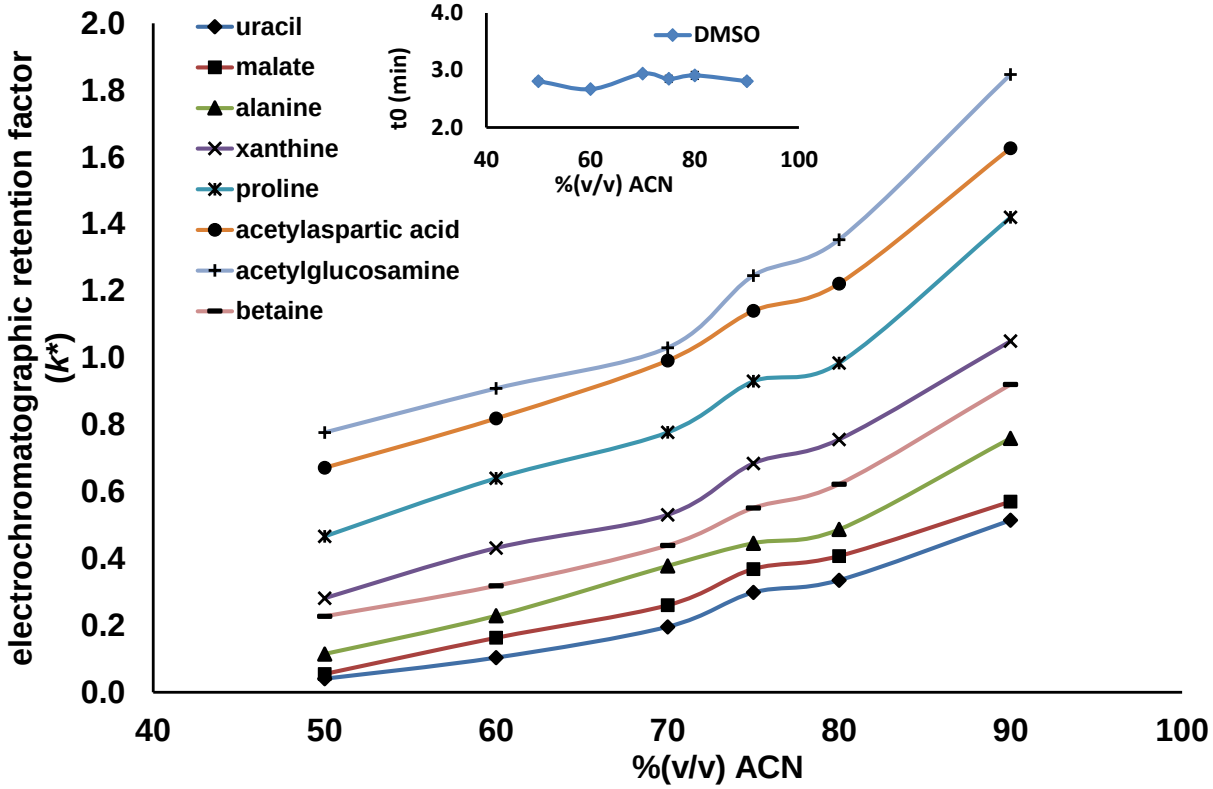

Figure 2.6 Effect of The of percent acetonitrile on retention factors of eight POC metabolites. Conditions: CEC-ESI-MS/MS using monolith poly (VBTA-co-BisGMA/EDMA). Experiment was performed on 60 cm(100 µm I.D.). Running buffer: ACN/water varies, 15mM heptflurobutyric acid, 5mM NH_4OAcpH= 1.8, Voltage: +15 kV; ; Capillary temperature, 20 °C. Injection: 5 kV 10s; ESI-MS conditions are the same as Figure 2.3.

2.4.2.3 Effect of Volatile BGE

As mentioned in the previous section, the use of volatile BGE as i mobile phase additive also had an influence on column performance. Two bases (TEA and BA), one salt (NH4OAC), and two acids (VA and HFBA) were used as mobile phase additives and tested at the optimum pH and % (v/v) of ACN. Figure 2.7 showed different resolution for the POC metabolites with different

additives. For example, the use of acid in the mobile phase showed better selectivity for two pairs of compounds, ALA/BET and BET/XAN. In addition, PRO/NAA acid pair was slightly better resolved using HFBA compared to the use of VA in the mobile phase.

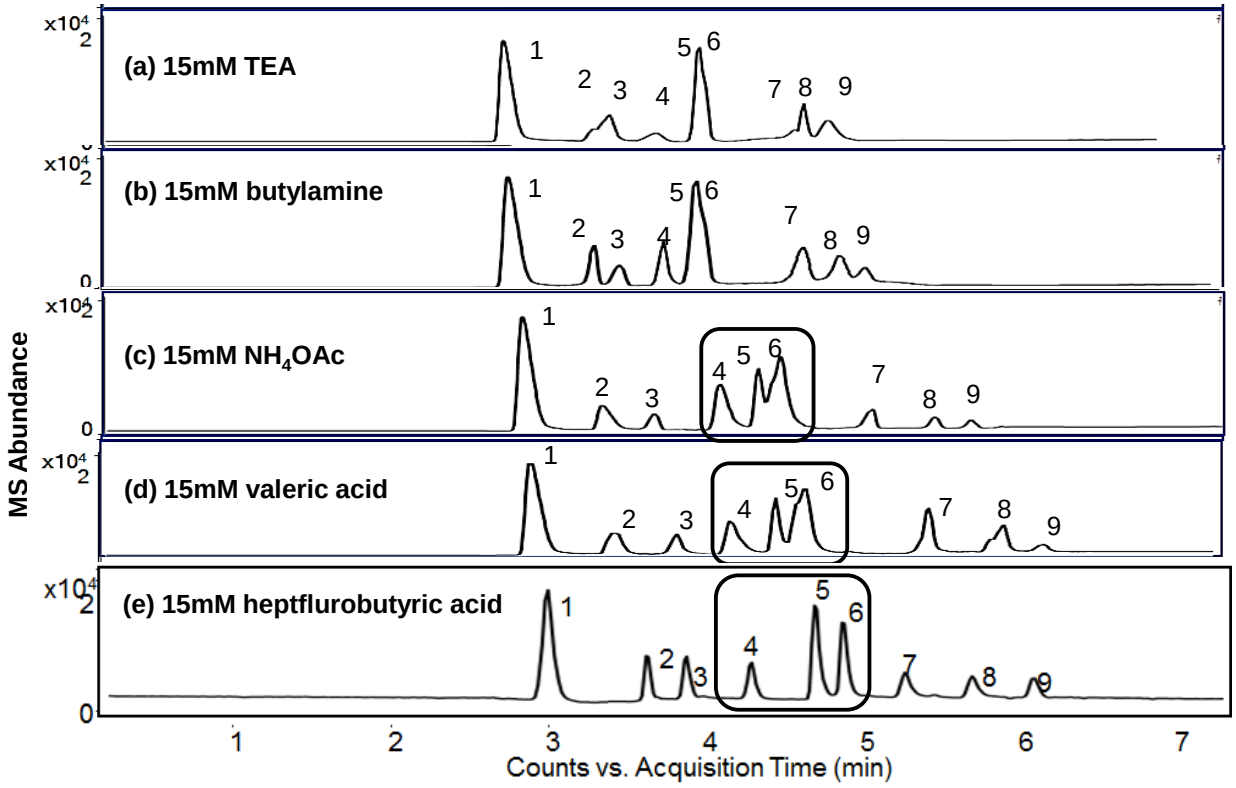

Figure 2.7 Effect of volatile mobile phase additives for on simultaneous separation of eight POC metabolites. Conditions: volatile additive was performed on 60 cm (100 μm I.D.) poly (VBTA-co-BisGMA/EDMA) monolithic column. Running buffer: ACN/water 75/25, additive varies, pH= 1.8, Voltage: +15 kV;Capillary temperature, 20 °C. Injection: 5 kV 10s; ESI-MS conditions are the same As Figure 2.3.

Furthermore, the use of acids provided slightly longer run time but overall better separation selectivity compared to the use of TEA, BA and NH_4OAC. The *S/N* of metabolites with different

types of additive in the mobile phase compared in Figure 2.8 shows that HFBA provides the highest *S/N*, resulting in us get lower LOD. Overall, the use of HFBA in the mobile phase could have baseline separation for all metabolites and less suppression of MS signal.

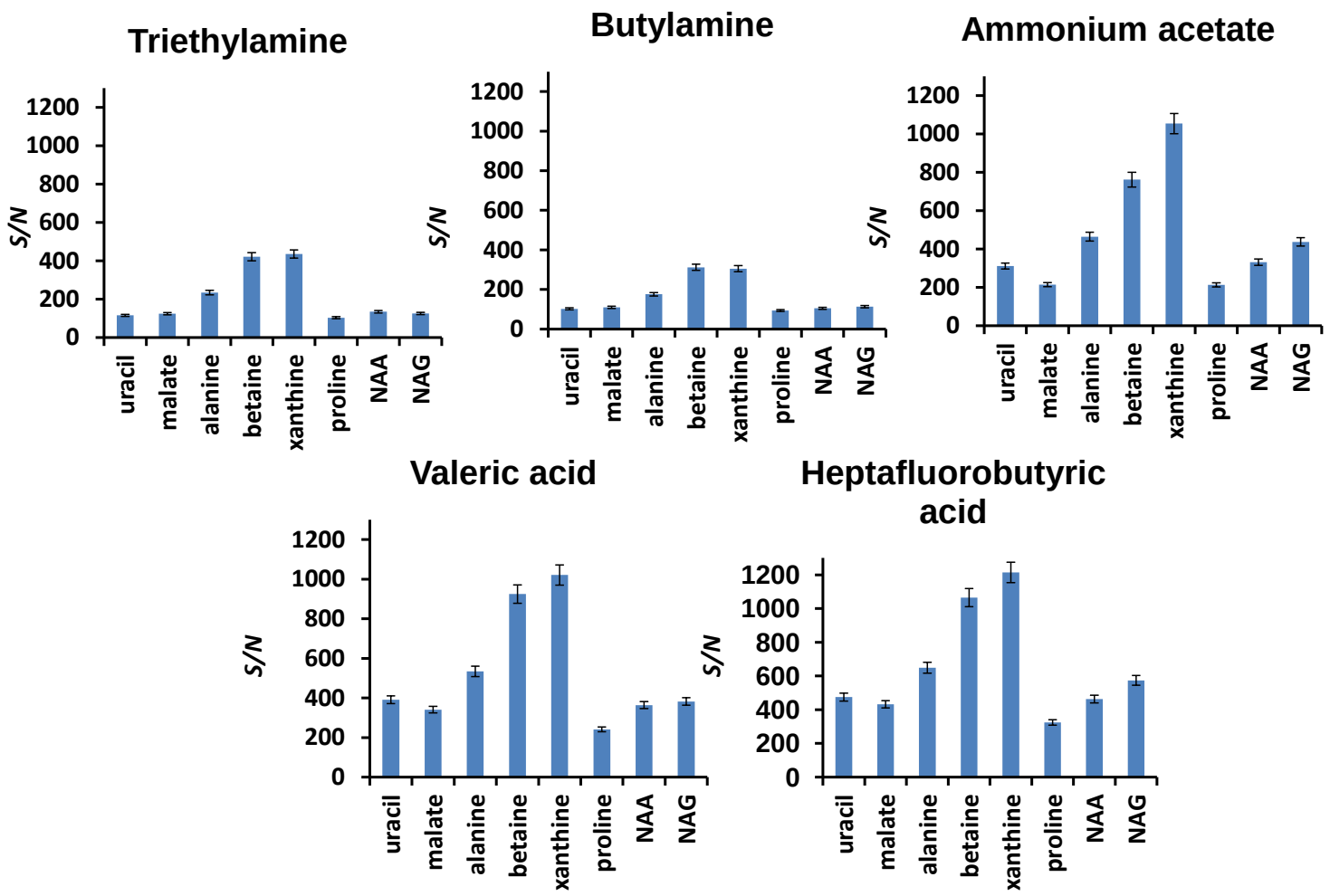

Figure 2.8 Effect of types of volatile additive in the mobile phase on S/N of eight POC in CEC-ESI-MS. Conditions: CEC-ESI-MS/MS using monolith poly (VBTA-co-BisGMA/EDMA) column 60 cm (100 μm I.D.). Running buffer: 75/25 ACN/water, 15mM heptflurobutyric acid, pH= 1.8, Voltage: +15 kV; Capillary temperature, 20 °C. Injection: 5 kV 10s; ESI-MS conditions are the same as Figure 2.3.

2.4.3 Comparison of CZE-MS, Open Tubular CEC-MS and Monolithic CEC-MS

A standard mixture of 8 POC metabolites was separated by monolith poly (VBTA-co-BisGMA/EDMA) CEC, VBTA coated CE (open tubular CEC) and bare silica CE. The comparison was performed in the optimized buffer condition for each column. Figure 2.9A shows the comparison of eight metabolites, in which the monolith poly (VBTA-co-BisGMA/EDMA) provided better separation selectivity and symmetrical peak shapes for metabolites mixture (Fig.9A) compared to CZE-MS or open tubular CEC-MS Although significant lower run times of POC metabolites were observed with CEC-MS and CZE-MS, the use of former provided separation of only DMSO (EOF marker peak) from the other eight metabolites, whereas the use of later provided only two distinct peaks. These results confirmed that CEC-MS with monolithic is a significantly useful tool to improve the separation selectivity of metabolites with very similar z/m.

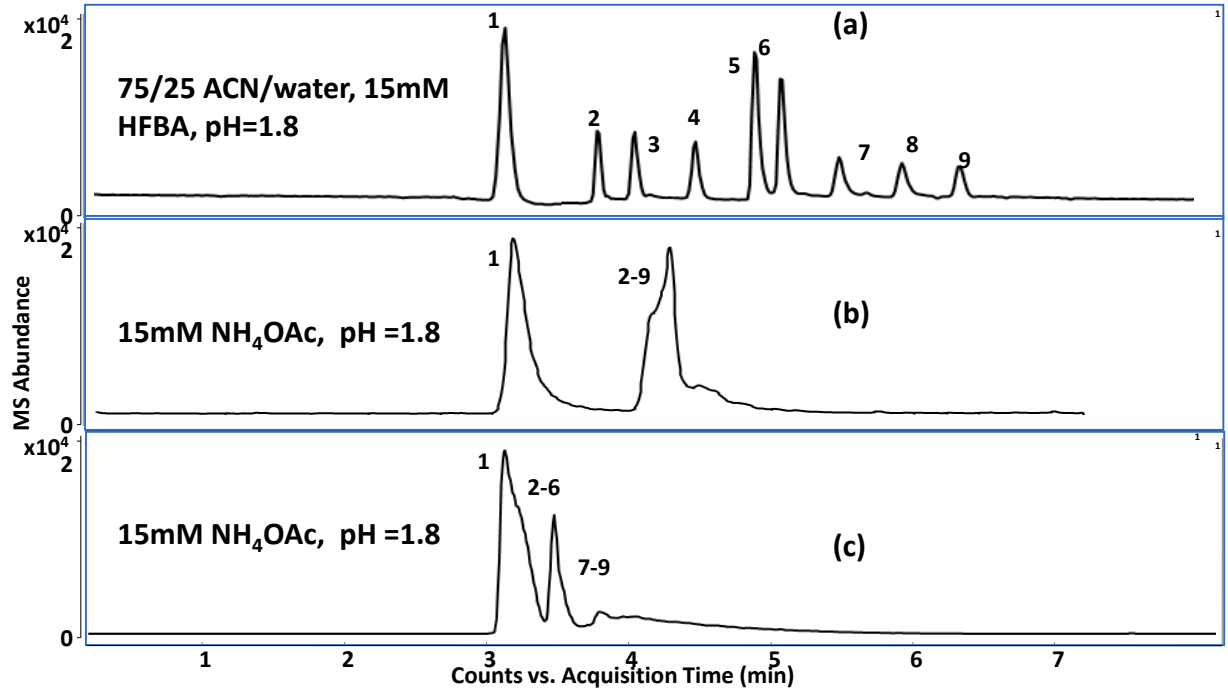

Figure 2.9 Comparison of the separation of 8 POC under optimized mobile phase on (a). VBTA monlotihic column, (b). VBTA coated column and (c).bare silica column. Conditions: (a). CEC-ESI-MS/MS using monolith poly (VBTA-co-BisGMA/EDMA). Experiment was performed on 60 cm (100 μm I.D.). Running buffer: 75/25 ACN/water, 15mM heptflurobutyric acid, pH= 1.8, Voltage: +15 kV; Capillary temperature, 20 °C. Injection: 5 kV 10s; ESI-MS conditions are the same as Figure 3; b). CEC-ESI-MS/MS using VBTA coated column. Running buffer: 15mM NH_4OAc, pH =1.8. Other conditions are the same as (a). (c). CE-ESI-MS/MS using bare silica column. Running buffer: 15mM NH4OAc, pH =1.8. Other conditions are the same as (a). Peak identification: (1) dimethylsulfoxide; (2) uracil; (3) malate; (4) alanine; (5) betaine; (6) xanthine; (7) proline; (8) *N*-acetylaspartic acid (NAA); (9) *N*-acetylglucosamine (NGG).

2.4.4 Comparison of Metabolites Separation with Varied Crosslinker Ratio

To test our hypothesis that hydrophilic interaction is the primary retention mechanism for metabolites, the CEC of POC metabolites were separated with two crosslinkers (EDMA-BisGMA) ratio. A comparison of chromatogram in Fig. Ten show that optimum ratio of BisGMA: EDMA is 5:15. Increasing the amount of hydrophilic crosslinker (BisGMA) compared the hydrophobic crosslinker (EDMA) decreased the separation of polar metabolites (Figure 2.10 C-D). In addition, the use of GMA or EDMA alone cannot provide separation of all eight polar metabolites. Thus,

Figure 2.10 confirmed our assumption that column B with a binary crosslinker ratio of 15:5 for EDMA: BisGMA is indeed the best monolithic column for CEC-MS separation. This column provided the desired peak shape, selectivity, and efficiency, compared to the use of other monolithic columns.

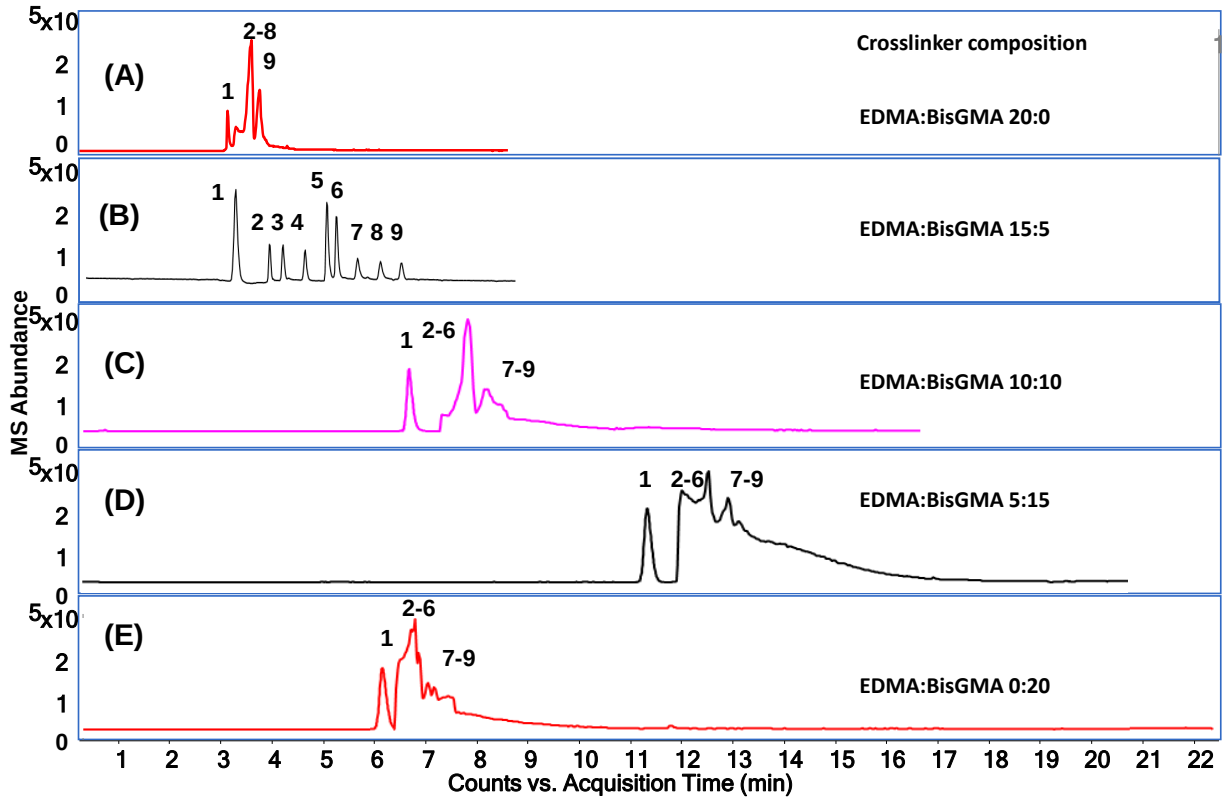

Figure 2.10 Chromatograms showing comparison of composition of crosslinker in the monolith. Conditions: CEC-ESI-MS/MS using monolith poly (VBTA-co-BisGMA/EDMA). Experiment was performed on 60 cm(100 µm I.D.). Running buffer: 75/25 ACN/water, 15mM heptflurobutyric acid, pH= 1.8, Voltage: +15 kV; Capillary temperature, 20 °C. Injection: 5 kV, 10 s; ESI-MS conditions are the same as Figure 2.3. Peak identification are the same as Figure 9.

2.4.5 Method Validation

2.4.5.1 Intraday and Interday Repeatability

Compared to LC-MS, CE-MS using open tubes has the disadvantage with unstable flow rate and somewhat poor repeatability of run times and *S/N*, due to capillary tip erosion when exposed to

the electrospray. Using the charged monomer VBTA, a stable and high EOF could be obtained to drive the mobile phase through the monolithic column bed. The top part of Table 2.2 shows intraday repeatability for 30 consecutive runs with a good % RSD of *tr* and *k** in the range of 1.6-4.6 and 1.4-3.7, respectively.

Table 2.2 RSD values for tr, k' and S/N for intraday (n = 30) study.

Compounds	% RSD t_R	%RSD *k*	% RSD *S/N*
uracil	1.6	1.4	2.9
malate	2.3	2.0	4.2
alanine	2.2	1.9	6.2
betaine	4.2	3.7	4.3
xanthine	3.9	3.5	3.5
proline	3.5	3.1	4.6
NAA	4.6	4.0	5.1
NAG	2.3	2.0	4.2

[1]Conditions: CEC-ESI-MS/MS using monolith poly (VBTA-co-BisGMA/EDMA) was performed on 60 cm (100 μm I.D.). Running buffer: 75/25 ACN/water, 15mM hepta flurobutyric acid, pH= 1.8; Other CEC-MS/ESI-MS conditions are the same as described in figure 6 (a).

The interday % RSD for three consecutive days (n =15 runs each day) for *tr*, *k** and *S/N* was found in the range of 1.6-4.6, 1.4-3.7 and 3.0-6.4, respectively (Table 2.3). As expected, the intraday and interday repeatability for *S/N* was slightly higher in the range of 2.9-6.2 and 3.0-6.4, respectively.

Table 2.3 RSD values for tr, k' and S/N for interday (n = 15, 3 days) study.

Compounds	% RSD t_R	%RSD *k*	% RSD *S/N*
uracil	1.6	1.4	3.0

malate	2.4	2.1	4.3
alanine	2.3	2.0	6.4
betaine	4.3	3.8	4.4
xanthine	4.1	3.5	3.6
proline	3.6	3.2	4.8
NAA	4.8	4.2	5.3
NAG	2.4	2.1	4.4

[1]Conditions: CEC-ESI-MS/MS using monolith poly (VBTA-co-BisGMA/EDMA) was performed on 60 cm (100 μm I.D.). Running buffer: 75/25 ACN/water, 15mM hepta flurobutyric acid, pH= 1.8; Other CEC-MS/ESI-MS conditions are the same as described in figure 6 (a).

The column to column repeatability experiment was carried out on three different monolithic columns with very good % RSD for *tr*, *k** and *S/N* in the range of 1.7-5.4, 1.5-4.7 and 3.4-6.5, respectively (Table 2.4). Interestingly, the % RSD for *S/N* for alanine is somewhat higher on the same column on three different days as well on three different columns on the same day suggesting the alanine signal was somewhat unstable in the electrospray compared to other polar analytes.

Table 2.4 RSD values for tr, k' and S/N for column to column (n = 15, 3 columns) precision study.

	% RSD	**%RSD**	**% RSD**
Compounds	t_R	***k***	***S/N***
uracil	1.7	1.5	3.4
malate	2.6	2.2	4.9
alanine	2.5	2.2	6.5
betaine	4.9	3.8	4.9

	% RSD	%RSD	% RSD
xanthine	4.6	3.6	4.0
proline	4.0	3.5	4.9
NAA	5.4	4.7	5.4
NAG	2.6	2.2	4.3

[1]Conditions: CEC-ESI-MS/MS using monolith poly (VBTA-co-BisGMA/EDMA) was performed on 60 cm(100 μm I.D.). Running buffer: 75/25 ACN/water, 15mM hepta flurobutyric acid, pH= 1.8; Other CEC-MS/ESI-MS conditions are the same as decribed in Figure 2.4.

2.4.5.2 Robustness

To examine whether the column performance would be affected by small variations in mobile phase and ESI-MS conditions, a robustness test was designed by using fractional factorial design (Dodde 11.0 software) The experimental multivariate design included the simultaneous investigation of five CEC-ESI-MS parameters (mobile phase pH, mobile phase ACN percentage, sheath liquid flow rate, nebulizer pressure and ESI voltage) were changed by 5% to 15% (Table 2.5).

Table 2.5 Fractional factorial design and the level of factors (Central, low, and high) values of each parameter chosen for the robustness study.

Factor	m.p. pH	m.p. ACN%	SL flow rate (uL/min)	Nebulizer Pressure (psi)	ESI voltage (V)
-1	1.5	66.5	7.6	6	3325
0	1.8	70	8	7	3500
1	2.1	73.5	8.4	8	3675

Factor	m.p. pH	m.p. ACN%	SL flow rate (uL/min)	Nebulizer Pressure (psi)	ESI voltage (V)
Factor Range	±15%	±5%	±5%	±15%	±5%

A total of 19 experiment were carried out, 11 trials were set at the middle of the investigational ranges and 8 trials were designed in combinations with the extreme values (Table 2.6).

Table 2.6 Fractional factorial design and experimental design and the corresponding response.

m.p. pH	% (v/v) ACN	SL Flow Rate	Nebulizer Pressure	ESI Voltage	S/N	Area	Resolution
1.5	66.5	7.6	8	3675	5864	6441	1.39
2.1	66.5	7.6	6	3325	5980	6432	1.35
1.5	73.5	7.6	6	3675	5861	6555	1.38
2.1	73.5	7.6	8	3325	5963	6541	1.37
1.5	66.5	8.4	8	3325	5847	6437	1.36
2.1	66.5	8.4	6	3675	5821	6455	1.35
1.5	73.5	8.4	6	3325	5803	6465	1.39
2.1	73.5	8.4	8	3675	5891	6421	1.37

The impact of the five parameters was estimated with three responses *Rs* of betaine/xanthine pair, *S/N* and peak area of betaine. Figure 2.11 shows the scaled and centered coefficients for the study output of *S/N*, peak area of betaine and the betaine/xanthine resolution. A confidence level of 99% was obtained with good % RSD of 4.2, 3.1 and 4.7 for *S/N*, *Rs* and peak area, respectively. In this coefficient plot, if the error bar falls into the parameter bar, it means this term is significant. In

our case, the positive error bars are much higher than the top of the parameter bar and negative error bars are much lower than the bottom of the parameter bar, which means the term is not significant. The figures illustrates that the small change does not make much difference to the separation and the detection.

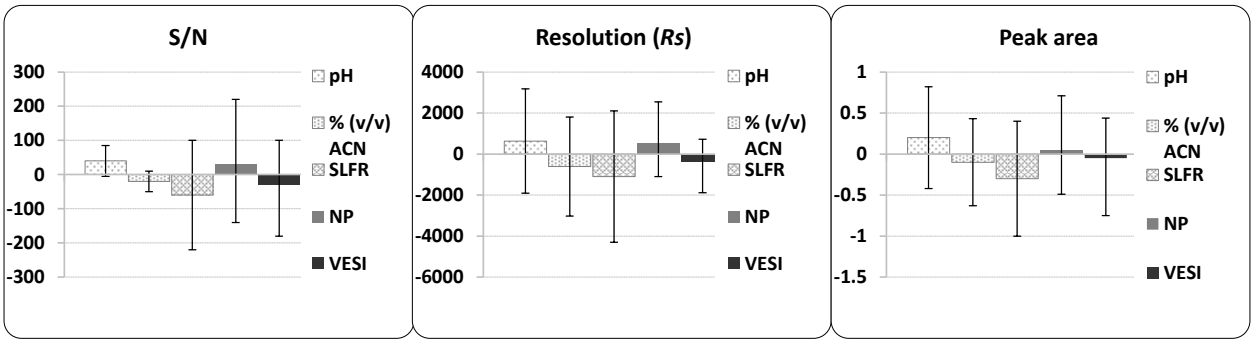

Figure 2.11 Scaled and centered coefficients for the studied outputs (S/N ratio, peak area, and resolution of betaine and xanthine) as a function of the parameters: pH, ACN%, SL flow rate (SLFR), nubulizer pressure (NP), ESI voltage (VESI).

A final consideration was to test the column lifetime for the repeatability of POC metabolite analysis. A series of 115 consecutive runs were performed on the monolithic column. The run-to-run repeatability was maintained with % RSD of less than 4.7. In addition, the peak asymmetry are maintained over more than one hundred consecutive analysis (Figure 2.12).

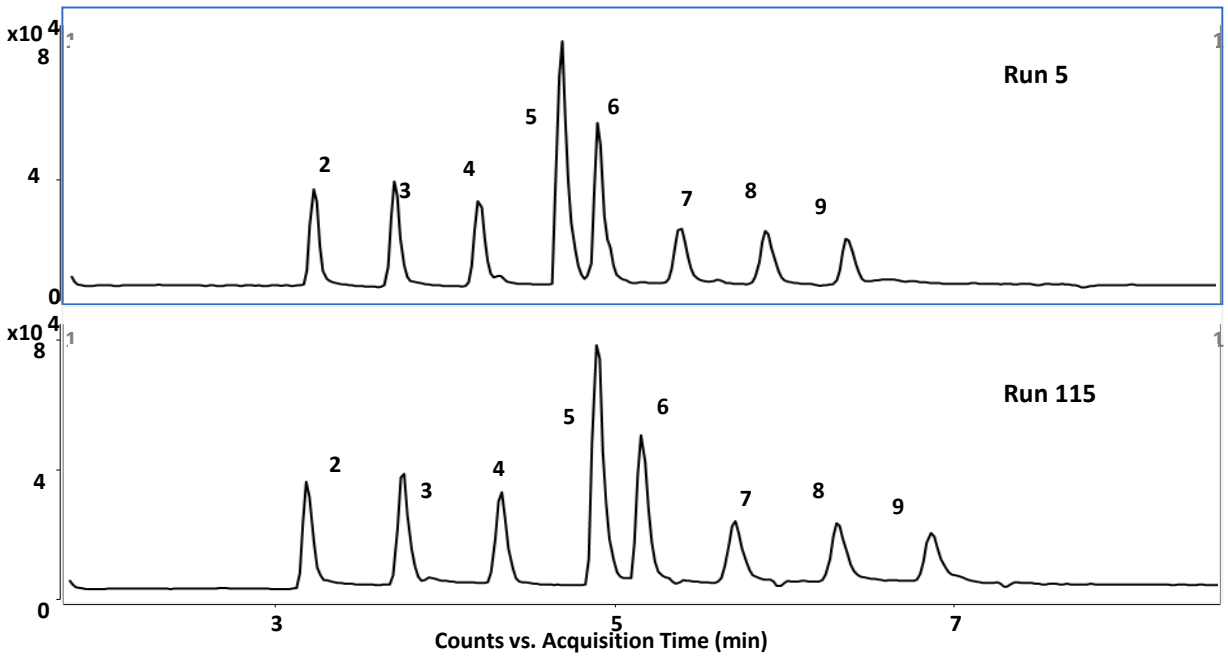

Figure 2.12 Column life time of poly-(VBTA-co-BisGMA/EDMA) monolithic columns. Separation of all eight POC metabolites were obtained by setting up automated 115 runs sequence on the CE 710 instrument

2.4.6 Analytical Figures of Merit

The quantitation of this study was performed with isotope labeled internal standards (IS). The calibration curves were obtained based on the peak area ratio between metabolites to IS versus the concentration of standard samples. Linearity of the calibration curve were tested in the range of 0.3-50 µM (Figure 2.7).

Compounds	Calibration curve	R^2	Linear range (µM)	LOD (µM)*	LOQ (µM)*
Alanine	y = 0.02169x + 0.0122	0.9996	0.3-50	0.05	0.25
Uracil	y = 0.0219x + 0.0097	0.9995	0.3-50	0.05	0.20

Compounds	Calibration curve	R^2	Linear range (µM)	LOD (µM)*	LOQ (µM)*
Betaine	y = 0.0205x + 0.0036	0.9996	0.3-50	0.05	0.10
Xanthine	y = 0.0212x + 0.0430	0.9990	0.3-50	0.05	0.10
Malate	y = 0.0019x -0.0007	0.9916	0.3-50	0.10	0.30
Proline	y = 0.0236x + 0.02377	0.9997	0.3-50	0.10	0.25
NAA	y = 0.0257x - 0.0014	0.9998	0.3-50	0.05	0.25
NGG	y = 0.02336x + 0.05431	0.9993	0.3-50	0.05	0.20

The linear regression were calculated using model equation y=ax+b, where x is the metabolites to IS peak area ratio and y is the analytes concentration. From the calibration curve, the correlation coefficient R^2 in the range of 0.9990-0.9998 for all analyte (except for malate). The LOD for most of metabolites was 50 nM except for malate and proline with LOD of 100 nM, due to the relatively low ionization and MS/MS response. A typical LOD chromatogram for all POC metabolites is shown in Figure 2.13. The LOQ for those metabolites is 100 nM-300 nM, which means this method is sensitive enough to quantitate almost all POC metabolites at nanomolar levels.

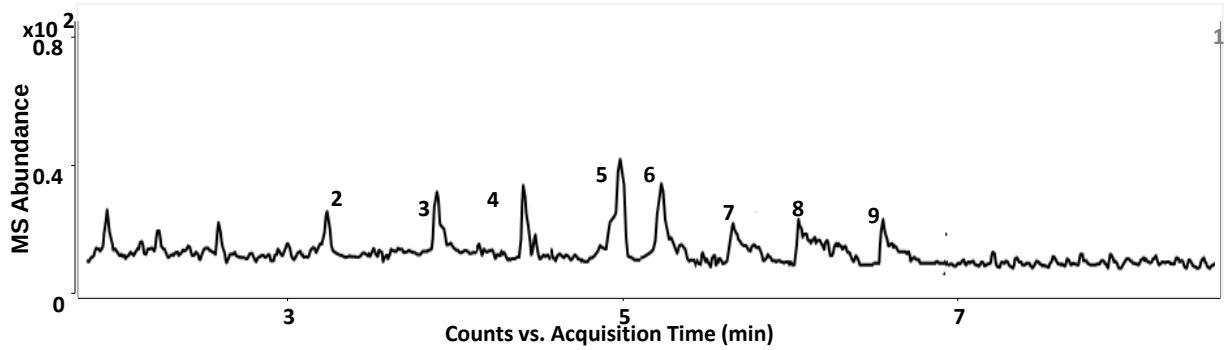

Figure 2.13 Chromatogram of metabolites separation of all eight POC metabolites at the limit of detection. Peak identification is the same as described in Figure 2.12.

2.4.7 Application to the Analysis of Biopsy Extracts of Prostate Tissue

Before quantitation of the POC metabolites in prostate tissue, the biopsy extracts were preconcentrated by ten folds. The procedure is shown in Figure 2.14. Briefly, each 0.6 mL of methanol extracted sample was transferred to a 1.5 mL vial and dried under a gentle air flow at room temperature for around 3 hours. The residue was reconstituted with 60 µL of 50/50 (v/v) MeOH /water in the same vials. The mixture was centrifuged for 20 min, and a 50 µL aliquot of the resulting supernatant was transferred to 200uL sample vial containing 10 L of IS at 500 M. Further addition of 20 L water and 20 L of methanol allowed the final volume for the

sample to be 100uL in 50/50 ACN /water.

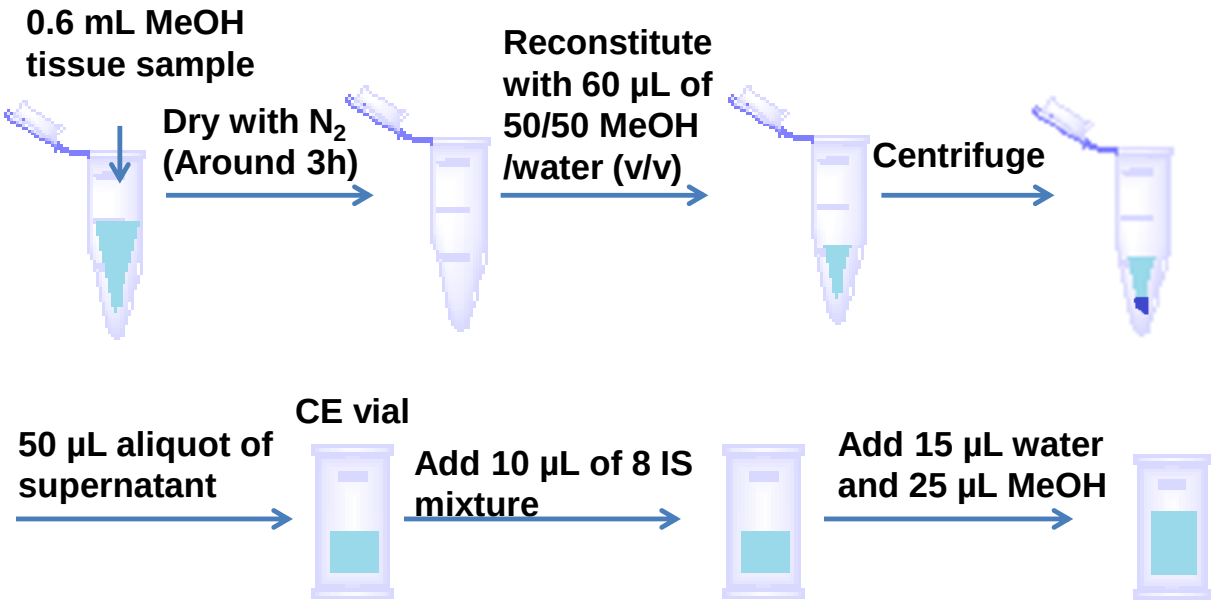

Figure 2.14 Prostate needle biopsy extracts preparation procedure.

The validated method and the calibration curve was used in the determination of POC metabolites concentration in prostate biopsy extract. The sample (extracted by mPREF) was provided by Dr. Dean Troyer's (Eastern Virginia Medical School). A total of 22-sample set as normal/tumor pairs were from the same patient. In this pair of sample, one sample is from the tumor containing part of prostate biopsy and the other one is from the healthy part of prostate. However, note that the classification of normal vs. diseased was unspecified and all samples were received in the coded form, and therefore this final analysis is considered as a blind test. Thus, we applied our validated method without knowing whether the sample is tumor containing or not. After we got the concentration data, the data was send back to EVMS for the clinical diagnostic results. At least 21 out of 22 pairs of sample match the clinic results and accuracy of 95.5% for this study is remarkable. A representative comparison chromatogram between two samples for one

normal/tumor pair is shown in Figure 2.15. As expected, each POC metabolites had higher *S/N* in tumor tissue compared to normal tissue.

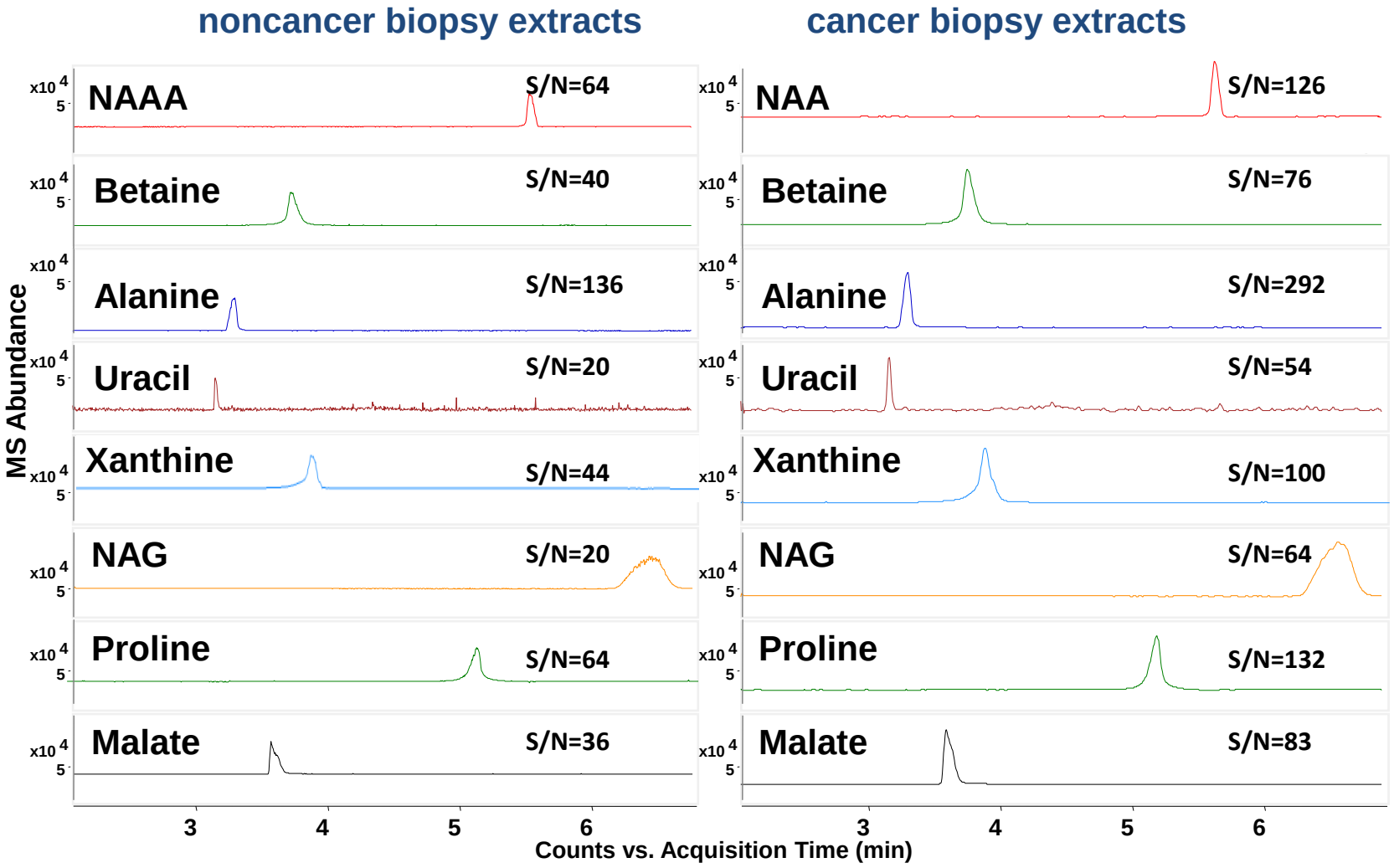

Figure 2.15 EIC chromatogram of metabolite distribution in biopsy extracts in cancer versus noncancer biopsy extracts.

One could easily tell the concentration difference between two paired sample with the bar plot in Figure 2.16. Two trends are obvious: First, concentration of all metabolites are higher in cancer vs. non-cancer human subjects. Second, concentration of two metabolites (alanine and proline) were highest among all metabolites irrespective of disease states.

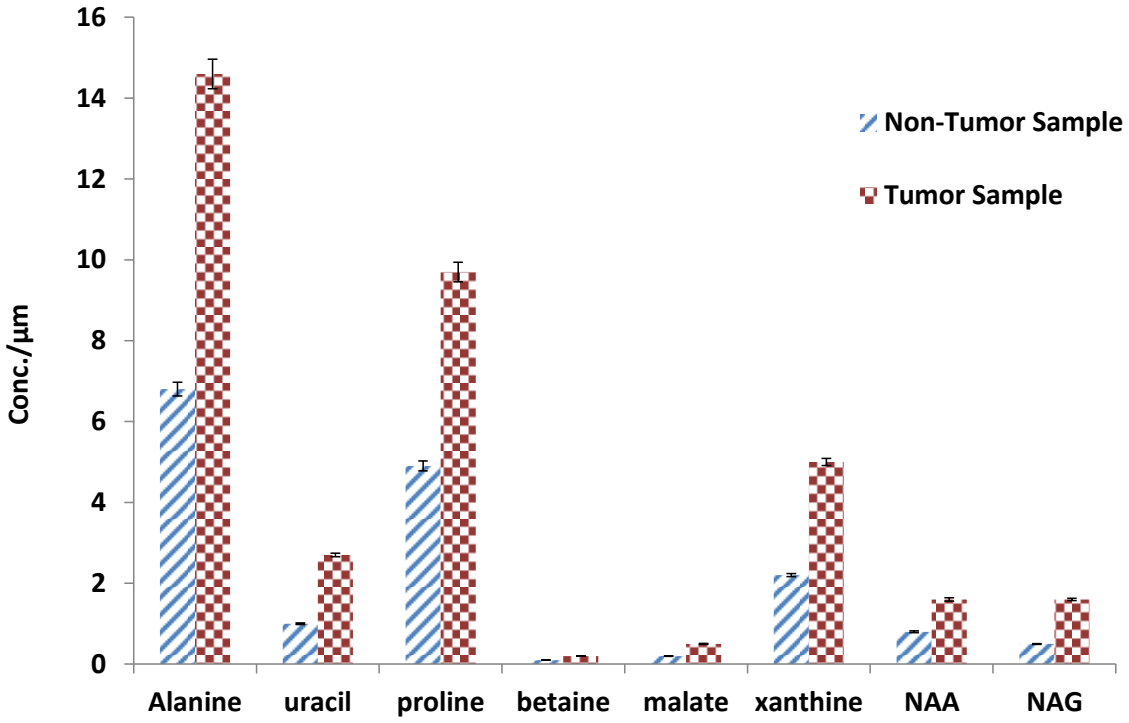

Figure 2.16 Concentration levels between normal vs. tumor biopsies extracts. Analysis Conditions are the same as Fig 2.5

A box plot of the concentration range between tumors versus normal prostate tissue extracts is shown in Fig. 17. Note that there is some overlap of concentration range between NEG and POS tumor group. This is mainly because the metabolites in this study not only participate the metabolism in prostate, but also involved in other pathways. For example, if a certain metabolite is active in other pathways of metabolism, the concentration of this metabolite may be higher in

this patient healthy prostate than other patient's tumor containing prostate biopsy.

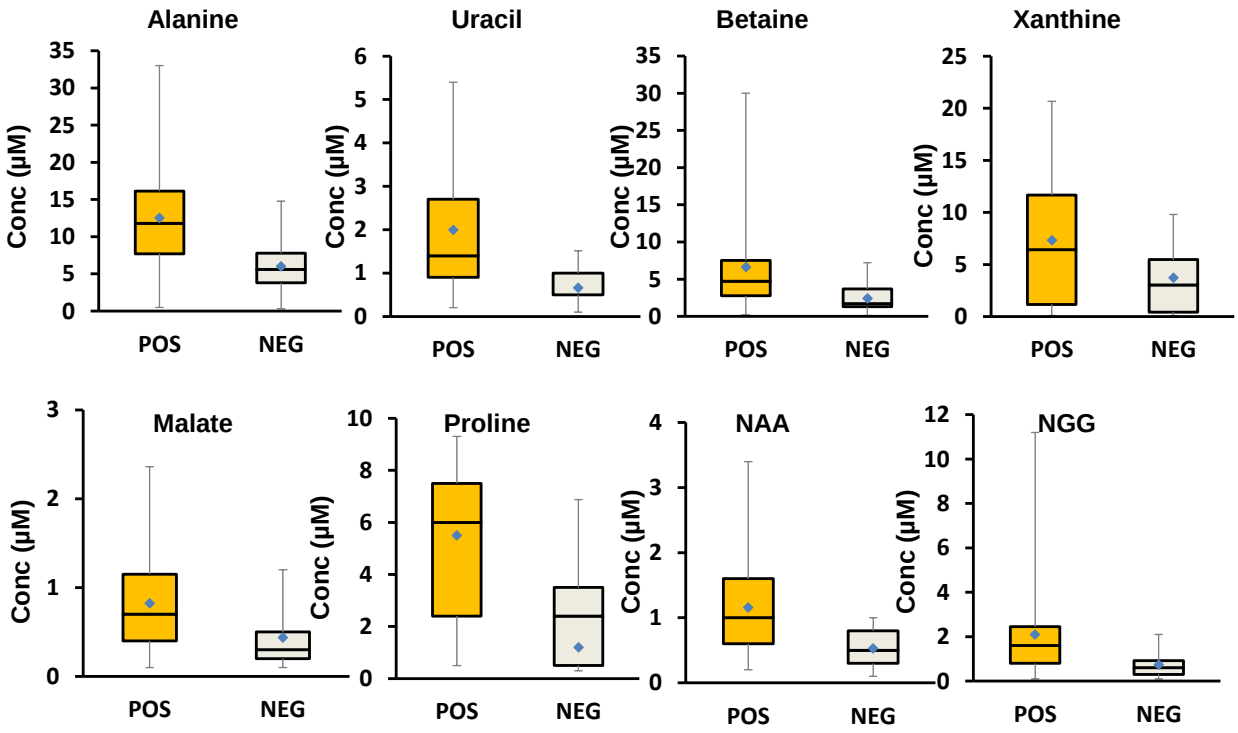

Figure 2.17 Box plots of tumor versus normal POC metabolite concentrations in biopsies extracts. POS indicates the presence of cancer; NEG indicated the absence of cancer; Study is based on 21 (tumor /non-tumor) pairs

2.5 Concluding remarks

A CEC-MS/MS platform for the quantitation of POC metabolites was successfully developed. First, the use of best monolithic column with favorable porosity and permeability was optimized. Second, to improve the separation selectivity of eight POC metabolites, mobile phase parameters (buffer pH, volume fraction of acetonitrile and buffer additive) were studied to improve the separation selectivity and S/N. Using 15mM HFBA in 75/25 ACN/water buffer at pH 1.8 baseline separation of all eight POC metabolites were achieved in less than 6.5 min. The combined use of a VBTA-*co*-BisGMA/EDMA monolith and a triple quadrupole MS provided a simple and

compatible hyphenation method with high repeatability of migration times and S/N for selective and sensitive MS/MS detection of all metabolites.

Compared to bare silica and open tubular coated column, the CEC-ESI-MS/MS method using the VBTA-*co*-BisGMA/EDMA monolith was the best method because it provided better separation selectivity, symmetrical peak shapes and more rugged CE-MS for analysis of POC metabolites mixture. The ruggedness studies performed suggest that there is potential to develop CEC-MS with monolithic column as an efficient diagnostic tool to routinely measure the concentration of small metabolites in biopsy extracts of prostate tissue samples.

References

(1) Brown, M. V.; McDunn, J. E.; Gunst, P. R.; Smith, E. M.; Milburn, M. V.; Troyer, D. A.; Lawton, K. A. *Genome medicine* **2012**, *4*, 33.
(2) Boda, D. *Curr. Proteomics* **2013**, *10*, 237-245.
(3) Ren, S.; Shao, Y.; Zhao, X.; Hong, C. S.; Wang, F.; Lu, X.; Li, J.; Ye, G.; Yan, M.; Zhuang, Z.; Xu, C.; Xu, G.; Sun, Y. *Molecular & Cellular Proteomics* **2016**, *15*, 154-163.
(4) Struck-Lewicka, W.; Kordalewska, M.; Bujak, R.; Mpanga, A. Y.; Markuszewski, M.; Jacyna, J.; Matuszewski, M.; Kaliszan, R.; Markuszewski, M. J. *Journal of Pharmaceutical and Biomedical Analysis* **2015**, *111*, 351-361.
(5) McGinnis, A. C.; Cummings, B. S.; Bartlett, M. G. *Anal Chim Acta* **2013**, *799*, 57-67.
(6) Guertin, K. A.; Moore, S. C.; Sampson, J. N.; Huang, W. Y.; Xiao, Q.; Stolzenberg-Solomon, R. Z.; Sinha, R.; Cross, A. J. *The American journal of clinical nutrition* **2014**, *100*, 208-217.
(7) Wu, Q.; Yu, X.; Wang, Y.; Gu, X.; Ma, X.; Lv, W.; Chen, Z.; Yan, C. *Electrophoresis* **2014**, *35*, 2470-2478.
(8) Wang, X.; Davis, I.; Liu, A.; Shamsi, S. A. *Electrophoresis* **2013**, *34*, 1828-1835.
(9) Bragg, W.; Shamsi, S. A. *J Chromatogr A* **2012**, *1267*, 144-155.
(10) Lin, X.; Feng, S.; Jia, W.; Ding, K.; Xie, Z. *J Chromatogr A* **2013**, *1316*, 104-111.
(11) Lu, Y.; Shamsi, S. A. *Journal of Chromatographic Science* **2014**, *52*, 1109-1120.

CHAPTER 3: Use of linear solvation energy relationships for capillary electrochromatographic retention: Application on Retention behavior and selectivity of neutral solutes on surfactant bonded monolith columns and insight into chiral recognition mechanism in enantioselective analysis

3.1 Abstract

As a useful tool linking the intermolecular interaction contribution to the retention of neutral molecules is linear solvation energy relationships (LSERs). This tool is known to predict the retention behavior and selectivity in high-performance liquid chromatography. This is a first article in which we propose to use LSERs to understand chiral recognition of amino acid based surfactant monolithic columns in CEC. This study includes two sections. In the first section, eight different amino based surfactant monomers were synthesized, with different chain length, linker type or head groups. Solutes retention behavior of a set of 31 neutral solutes were characterized and compared using LSER. . The system parameters (aka. system coefficients) of eight monolithic columns were characterized and the results indicate that the LSER is an excellent approach to the selectivity of neutral compounds for capillary electrochromatography (CEC). In the second section, one of the chiral monolithic column, poly (AADCL-*co*-EDMA was chosen, and a set of seventeen chiral compounds were screened on this chiral stationary phase (CSP). Next, the A-V descriptors of a set of 17 chiral compounds along with the system coefficient of poly (AADCL-*co*-EDMA) was used to calculate the separation factor (i.e., k' predicted). At least six out of 17 chiral compounds were found to have k' predicted of the second eluted enantiomer generated by LSER equation matched with the experimental retention factor value. By calculating the delta x system of coefficients of six molecular enantiomers, it was possible to predict the enantioselectivity which

was found to be an excellent agreement with the experimental determined enantioselectivities. This study indicated the possibility to use LSER as a potential tool to get insights into chiral recognition mechanism.

3.2 Introduction

Linear solvation energy relationships (LSERs) are relationships between solute retention behavior and the numerical measures of analytes properties. The LSERs equation are routinely used to understand the relationships between molecular interactions that control the retention and selectivity in gas chromatography (GC), high performance liquid chromatography (HPLC), supercritical fluid chromatography (SFC) and micellar electrokinetic chromatography (MEKC).

The aim of LSERs studies in chromatography is to understand the intermolecular processes controlling retention. By generating LSERs model, we could predict the experimental retentions quantitatively to achieve an acceptable separation. To systematically characterize stationary phase in chromatographic studies, a thermodynamic parameter, i.e. the solute retention factor in the form of log *k'*, is used, which associates with the solute descriptors in a given separation system using system constants (aka. system parameters). These coefficients measures the magnitude of difference between the stationary phase and the mobile phase but the solute descriptors are independent of the chromatographic system. Numerous tables of solute descriptors have been published.[1] Chromatographic system (mobile and stationary phase, temperature) is calibrated using solutes with known descriptors to establish its system parameters. Once the later are known, the retention factors of any solute whose LSERs descriptors are unknown can be predicted. Equation (1), which is one of the more widely accepted equation forms of the LSERs model is expressed as follows:

$$logk = c + eE + sS + aA + bB + vV \quad (1)$$

in which k is the solute retention factor ($(t_R - t_0)/t_0$). In the above equation, the capital letters *A, B, E, S* and *V* are the solute descriptors, whereas the lower-case letters (*a, b, e, s* and v) are the system constants. As mentioned earlier, the A-V solute descriptors are only related to the solute and independent of the mobile and/or the stationary phase used. On the other hand, a-v system constants reflects the difference in solute interactions between the mobile phase and the stationary phase. Figure 3.1 is a cartoon picture showing a LSERs. The capital letter *A* represents for the solute hydrogen bond acceptor ability, whereas *B* is the solute hydrogen bonding accepting ability. Thus, the overall aA and bB terms are H-bond interactions, *a* is the system parameter for basicity interactions with acidic *A* solutes and *b* is the system parameter of acidity interactions with basic B solutes. The *E* descriptor represents for the molar refraction due to n or/and π electrons in the molecule structure. Hence, the *eE* term represents polarizibility (induced dipole) type interactions. The term *S* is the solute descriptor for the polarizability and dipolarity of the molecule. Hence, the *sS* term is a component of polarizibility interactions. The fifth descriptor, *V* stands for the molecular cavity formation energy, calculated using the solute structure.[2] Thus, the overall term *vV* represents hydrophobic or dispersive interactions.

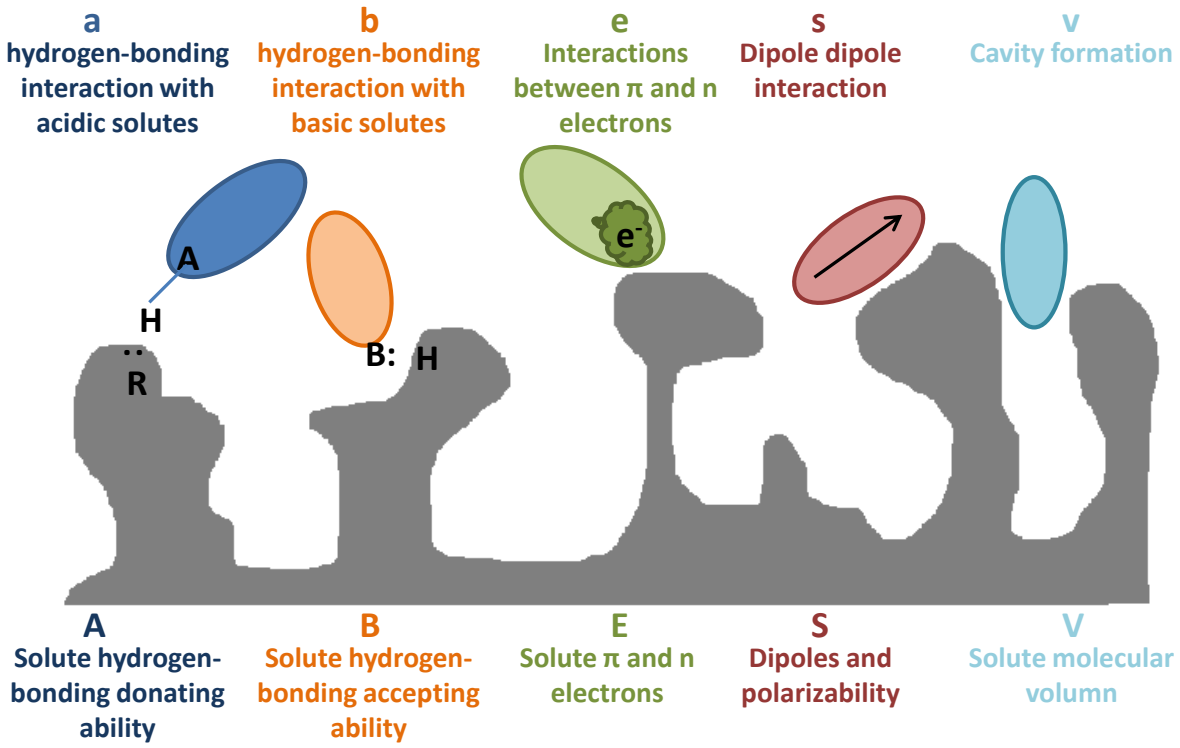

Figure 3.1 Linear solvation energy relationship model: solute descriptors and interactions related to stationary phase. The monolithic stationary phase is marked in grey color and the interaction (retention) of the stationary phase is characterized by measuring the sum of system coefficients (represented by lower case letters a,b, e, s and v) at the top , and solute descriptors (represented by upper case letters, A, B, E, S and V) at the bottom.

In the LSERs, two enantiomers share the same solute descriptor values, which means the enantiomers would not be separated by achiral stationary phase. Instead, enantiomers could be separated on a chiral stationary phase (CSP). As mentioned by Mitchell et al.[3-6], the less retained enantiomer of the enantiomeric could be considered as reference solute to model the enantioselectivity factor α using modified the LSERs equation as follows,

$$logk_2 - logk_1 = log\alpha = \Delta eE + \Delta sS + \Delta aA + \Delta bB + \Delta vV \qquad (2)$$

in which, k_1 and k_2 are the retention factors of first and second eluting enantiomer, respectively. The ΔxX terms indicate the difference of enantiomer/CSP interactions. As this equation is based

on the difference of intermolecular interactions for enantioselectivity, good understanding on equation 2 could give an insight into the chiral recognition mechanism and predict whether chiral compounds could be separated on certain chiral stationary phase (CSP).

In the first part of this project, retention measurements of 31 achiral solutes have been carried out on eight amino acid bound monolithic CSP. The chain lengths, head group, and linker types are compared to evaluate similarities and differences among these CSPs for the determination of LSERs system parameters or system constant. The original column poly (10-acryl-amidodecenoxy carbonyl-L-leucine-*co*-EDMA) column was made by our group with an amino acid surfactant serves as chiral monomer of CSP.[7] A set of different amino acid surfactant were synthesized are used as monomer in the formation of surfactant bound polymer monolithis. The chemical structure of eight surfactants 8-acrylamidooctenoxy carbonyl-L-leucine (AAOCL), 10-acryl-amidodecenoxy carbonyl-L-leucine (AADCL), and 12-acryl-amidododecenoxy carbonyl-L-leucinate (AADoCL), 10-acryl-amidodecenoxy carbonyl-L-alanine (AADCA), 10-acryl-amidodecenoxy carbonyl-L-valine (AADCV), acrylamidoundecanoyl-L-alanine (AAUA), acrylamidoundecanoyl-L-valine (AAUV) and acrylamidoundecanoyl-L-leucine (AAUL) are shown in Figure 3.2 and was originally reported by Shamsi's group.[7]

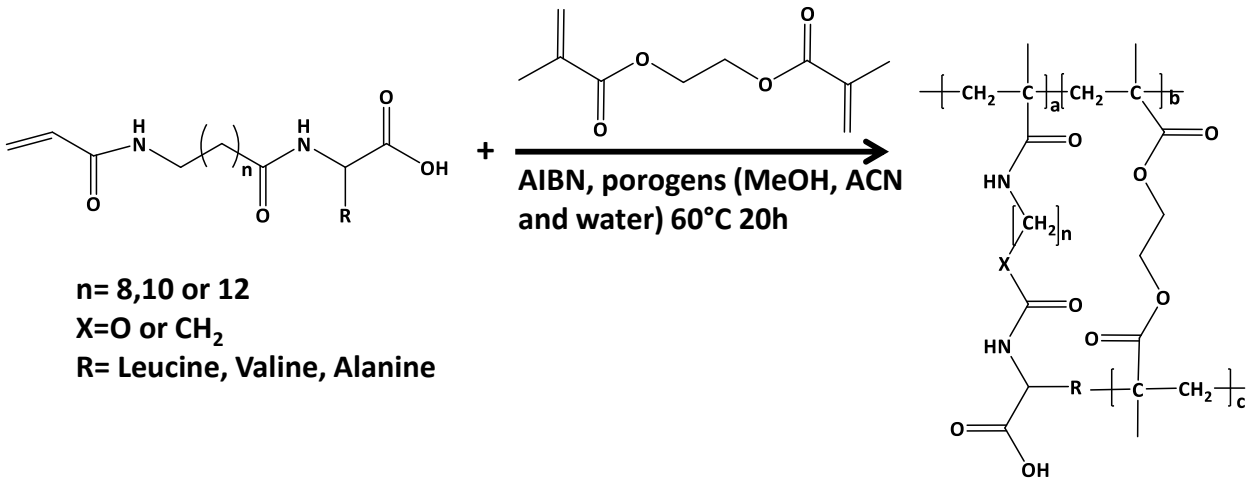

Figure 3.2 scheme for polymerization of amino acid based surfactant monolithic column. 8 columns used in this study are as follows: poly-(AAOCL-*co*-EDMA), poly-(AADCL-*co*-EDMA), or poly-(AADoCL-*co*-EDMA) monoliths with monomer linker X=C, head group R=leucine, and carbon number n = 8, 10, and 12, respectively; poly-(AADCV-*co*-EDMA) and poly-(AADCA-*co*-EDMA) monoliths with monomer linker X=C, carbon number n = 10, and head group =valine and alanine, respectively; poly-(AAOCV-*co*-EDMA) and poly-(AAOCA-*co*-EDMA) and poly-(AAOCL-*co*-EDMA) monoliths with cross linker X=O, carbon number n=8, head group R=valine, alanine and leucine, respectively. The letters , b, c, m and n are the aggregation numbers.

The interactions, contribustion to enantioseparation is discussed in section II. Thus, in the seond part of this project, 42 chiral compounds were screened on poly-AADCL-co-EDMA column and 17 chiral compounds were separated. The experimental retention factor value of two enantiomers will be compared to the predicted retention factor value, which is calculated by the LSERs equation generated in part one. As most chiral compounds are ionic in pH 5.0 mobile phase, a modified equation was used.

$$k^* = \frac{k' - \mu_{ep} / \mu_{eo}}{1 + \mu_{ep} / \mu_{eo}} \qquad (3)$$

In which k* is the electrochormatographic retention factor, μ_{ep} is the electrophoretic mobility and μ_{eo} is the electroosmotic mobility. [8]

If one enantiomer has identical value of predicted and experimental retention factor, the other enantiomer's retention factor and solute descriptors could be used to generated a second LSERs equation, which means the enantiomers are considered to interact with different CSP domains.[9]

Capillary electrochromatography (CEC) combines the excellent selectivity of high-performance liquid chromatography (HPLC) with the superior efficiencies of capillary electrophoresis (CE). Varied stationary phase in CEC includes packed column, coated column, silica-based and polymer-based monolith columns. Due to the high permeability, high surface area for reactivity, high repeatability and flexible choice of function group on CSP, polymer-based monolith column were chosen for this study. [7,10,11] The aim of this work is to develop a retention model for the characterization of eight amino acid surfactant bound monolithic columns. Furthermore, we selected AADCL as a model monolithic column to evaluate chiral interactions because previous work in Shamsi's group has shown good chiral selectivity for this particular monolithic column.[7]

3.3 Experimental

3.3.1 Reagents and Materials

2,2′-azobis(2-methylpropionitrile) (AIBN), 3-(trimethoxy-silyl)propyl methacrylate (γ-MAPS), 10-amino-1-decanol, 8-amino-1-octanol, 12-amino-1-dodecanol, and triphosgene were obtained from TCI-America (Portland, OR). Ethylene glycol dimethacrylate (EDMA) purchased from Sigma-Aldrich was distilled to remove inhibitor before its usage. The HPLC grade acetonitrile (ACN), methanol (MeOH), triethylamine (TEA) and 7.5 M ammonium acetate (NH_4OAc) aqueous solution, dimethyl sulfoxide (DMSO), benzene, toluene, ethylbenzene, propylbenzene, butylbenzene were purchased from Sigma-Aldrich (St. Louis, MO). Other chemicals used for the synthesis of surfactant monomer, such as pyridine, anhydrous Na_2SO_4, L-leucine,

dichloromethane, sodium bicarbonate, sodium hydroxide, hydrochloric acid, and ethyl acetate were also purchased from Sigma-Aldrich. Ethanol (HPLC grade) was purchased from Fisher Scientific (Fair Lawn, NJ). Triply deionized water (18.2 MΩcm) was generated in the laboratory using Barnstead Nanopure II Water System (Dubuque, IA). The achiral and chiral compounds used in this study were purchased from Sigma-Aldrich. All the chemicals have the purity of 98% or higher and were used as received without further purification unless specifically noted.

3.3.2 Preparation of Monolithic Columns

A 40 cm long fused silica capillary (360 μm o.d., 100 μm i.d., Polymicro Technologies, Phoenix, AZ) was flushed under vacuum with acetone and 1 M NaOH for 15 min each. The capillary was then filled with 1 M NaOH and both ends were sealed with rubber septa and heated at 100 °C for 2 h in a GC oven. Next, the capillary was flushed with triply deionized water, 1 M HCl, triply deionized H_2O, and MeOH for 15 min each under vacuum. A solution of γ-MAPS (50%, v/v in anhydrous MeOH) was then filled through the capillary under vacuum. The filled capillary was once again sealed with rubber septa and kept at 50 °C for 14 h in a GC oven. Next, the unreacted γ-MAPS solution was removed by flushing the capillary under vacuum using acetone for 5 min. The vinylized capillary was eventually dried by nitrogen for 3 h at 60 °C in a GC oven.

A typical procedure for making AADCL monolithic columns is described as follows. First, 15 mg of AADCL and 0.5 mg of AIBN were dissolved in a mixture containing various compositions (% wt/wt) of dimethyl ether, ACN, MeOH, and H_2O as porogens. To each of the porogen mixture, 14.3 μL of EDMA was added. The final polymerization solution was ultrasonicated for 30 min and filled into the pretreated capillary using a hand held syringe. Typically, in the preparation of CEC-UV column, 30 cm out of 40 cm of the pretreated capillary was filled. The column was then

sealed with rubber septum and was kept at 60 °C to polymerize. After 20 h of polymerization, the column was flushed with ACN for ~2 h to remove the unreacted monomers. The on-column detection window was then burned in the empty segment of the capillary adjacent to the packed monolithic bed and 8.5 cm to the outlet end of the capillary for CEC-UV experiment. The column was eventually cut to obtain a total length of 33.5 cm with a monolithic bed of 25 cm (from the inlet end). The monolithic capillary was conditioned for 24 h with running buffer before use.

3.3.3 Instrumentation

Agilent CE station(Agilent Technologies, Palo Alto, CA) equipped with an auto sampler, 0-30 kV power supply, and a diode-array UV detector was used to carry out all the CEC experiment. Agilent 3D-CE ChemStation software (Rev. A. 08.04) was used for data acquisition and analysis. A series III isocratic HPLC pump (Lab Alliance, State College, PA) was used to flush and condition the column. An Ultra-Plus II micro-HPLC system (Micro-Tech Scientific Inc., Fontana, CA) was used for the measurement of porosity and permeability. All LSERs modeling were performed on SAS (9.3).

3.4 Results and Discussion

3.4.1 Achiral Solutes and LSERs Equation Generation

The retention behavior of 31 achiral test solutes was examined in each monolithic column and compared to generate the LSERs model. Due to the high UV absorption, a set of benzene derivative with known molecular descriptors (Table 3.1) were chosen to determine system constants of Eq. 1 for the eight monolithic columns.[12] Based on the solute descriptor value on hydrogen bonding ability (parameters *A* and *B*), the solutes are divided into 3 sets, hydrogen bond donors (HBDs) (*A* ≥B), nonhydrogen bond donors (NHBs) (*B* ≤0.20) and hydrogen bond acceptors (HBAs) (solutes

13-23, $B \geq 0.22$).[13] trends for HBD, NHB and HBA solutes are showin in a series of electropherograms in Figure 3.3-3.4, C1-C4. The effect of chain length of monolithic column on separation of HBD is shown in Figure 3.3.

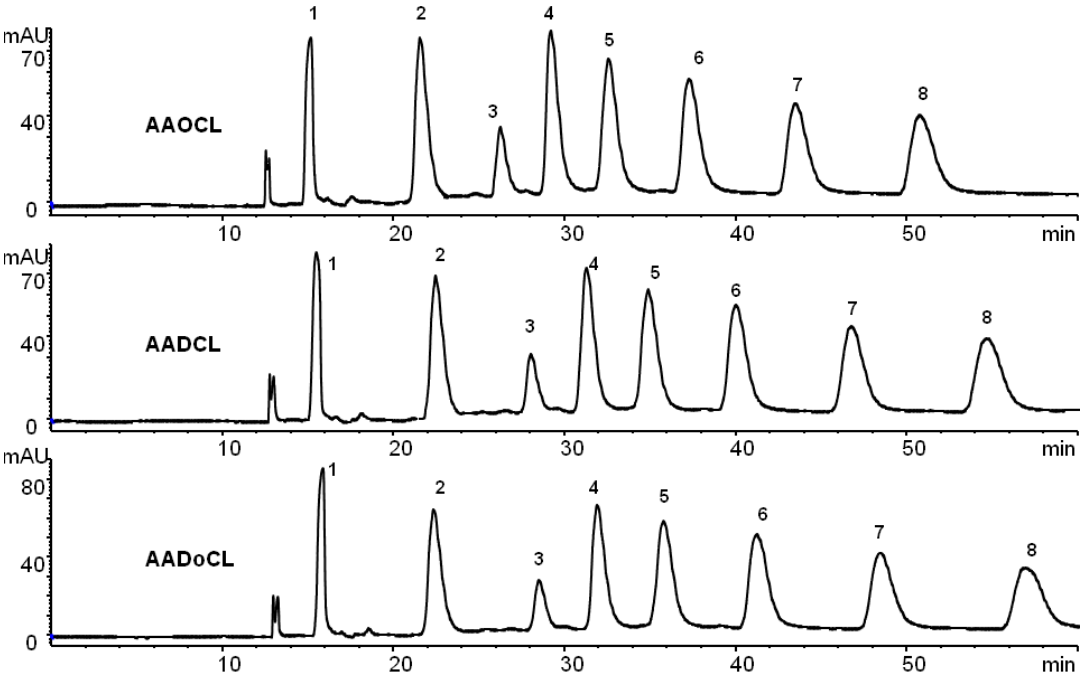

Figure 3.3 Effect of chain length of monolithic column on separation of hydrogen bond donors (HBD). Peak identification: (1). benzyl alcohol, (2). phenol, (3). 4-ethylphenol, (4). 4-fluorophenol, (5). 4-chloropheno, (6). 4-bromopheno, (7). 3-chlorophenol, (8). 3-bromophenol.

With the increase in carbon chain length from 8 to 12, the retention of all HBD solutes increase without any alteration in separation selectivity. Effect of the head group and -linker type of the monolithic column on separation of HBD is shown in Figure 3.4.

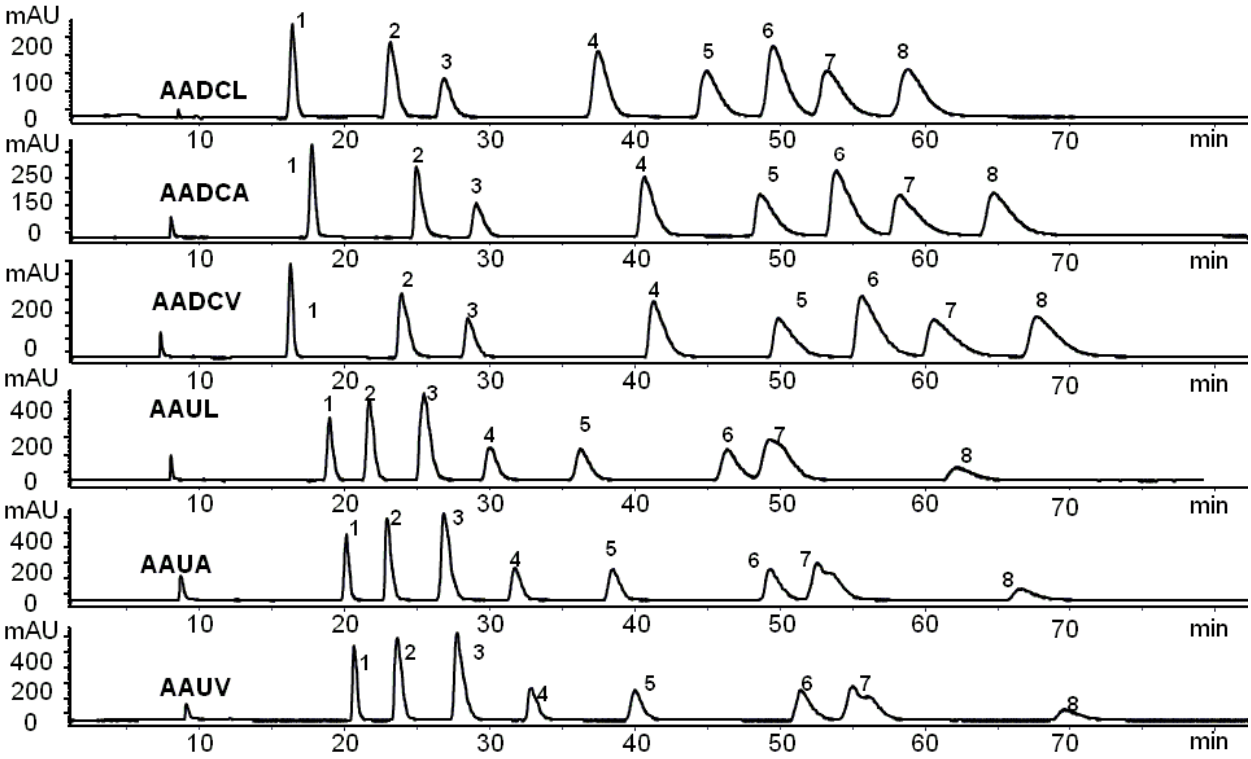

Figure 3.4 . Effect of head group and linker types of surfactant-bound monolithic column on separation of hydrogen bond donors (HBD). Peak identification: (1). benzyl alcohol, (2). phenol, (3). 4-ethylphenol, (4). 4-fluorophenol, (5). 4-chloropheno, (6). 4-bromopheno, (7). 3-chlorophenol, (8). 3-bromophenol.

By comparing the retention of solutes with same monomer head group but different cross-linker, a conclusion could be made that the surfactant linker containing oxygen has less retention on the solutes than linker with methylene groups. With the carbamate linker, the hydrophobicity of the monolithic column is higher than the amide monomer. As a result, the retention of achiral solutes are longer in carbamate (AADCL, AADCV, and AADCA) monolith over amide (AAUL, AAUV, and AAUA) monolith. The monomers head groups (leucine, alanine, and valine) have ascending retention to the solutes. The same trend was found on NHB solute sets (Figure C1-C2) and HBA (Figure C3-C4).

This is mainly because of the structure and molecular volume difference of head group. With DMSO as the t_0 marker, retention factor of all solutes were calculated. Using the solute descriptor values tabulated in in Table 3.1, the LSERs equation coefficients for eight different stationary phase were calculated. All coefficients are discussed separately under a subheading in the order it is mentioned in LSER equation (1).

Table 3.1 Solute descriptors of 31 achiral compounds.

		V	S	A	B	E
Solute descriptors	**Nonhydrogen bond donors (NHD)**					
1	Benzene	0.716	0.61	0.52	0	0.14
2	Toluene	0.857	0.601	0.52	0	0.14
3	Ethylbenzene	0.998	0.613	0.51	0	0.15
4	Propylbenzene	1.139	0.604	0.5	0	0.15
5	p-Xylene	0.998	0.613	0.52	0	0.16
6	Chlorobenzene	0.839	0.718	0.65	0	0.07
7	Bromobenzene	0.891	0.882	0.73	0	0.09
8	Iodobenzene	0.975	1.188	0.83	0	0.12
9	4-Chlorotoluene	0.98	0.705	0.67	0	0.07
10	Biphenyl	1.324	1.36	0.99	0	0.22
11	Naphthalene	1.085	1.36	0.92	0	0.2
12	1-Methylnaphthalene	1.226	1.344	0.9	0	0.2
	Hydrogen bond acceptors (HBA)					
13	Acetophenone	1.014	0.818	1.01	0	0.48
14	Benzonitrile	0.871	0.742	1.11	0	0.33
15	Methyl benzoate	1.073	0.733	0.85	0	0.46

		V	S	A	B	E
16	Ethyl benzoate	1.214	0.689	0.85	0	0.46
17	4-Chloroanisole	1.038	0.838	0.86	0	0.24
18	4-Nitrotoluene	1.032	0.87	1.11	0	0.28
19	4-Chloroacetophenone	1.136	0.955	1.09	0	0.44
20	Methyl 2-methylbenzoate	1.214	0.772	0.87	0	0.43
21	Phenyl acetate	1.073	0.661	1.13	0	0.54
22	3-Methylbenzyl alcohol	1.057	0.815	0.9	0.33	0.59
23	Phenethyl alcohol	1.057	0.784	0.83	0.3	0.66
	Hydrogen bond donors (HBD)					
24	Benzyl alcohol	0.9160	0.8030	0.8700	0.3300	0.5600
25	Phenol	0.7750	0.8050	0.8900	0.6000	0.3000
26	4-Ethylphenol	1.0570	0.8000	0.9000	0.5500	0.3600
27	4-Flourophenol	0.7930	0.6700	0.9700	0.6300	0.2300
28	4-Chloroaniline	0.9390	1.0600	1.1300	0.3000	0.3100
29	4-Bromophenol	0.9500	1.0800	1.1700	0.6700	0.2000
30	3-Chlorophenol	0.8980	0.9090	1.0600	0.6900	0.1500
31	3-Bromophenol	0.9500	1.0600	1.1500	0.7000	0.1600

3.4.2 System parameters for chiral monolithic columns

Table 3.2 compares the system parameters obtained for eight monolithic columns with different chain lengths (AAOCL, AADCL, AADoDCL), head groups (AADCL, AADCV, AADCA) and linker type (AADCL vs. AAUL). In LSERs equation, a larger value of coefficient associated with each descriptor represents a stronger interaction between solutes and stationary phase or mobile

phase. For example, solute-stationary phase interactions are positive for positive coefficient values whereas solute-mobile phase interactions are negative for negative coefficient values associated with the solute descriptors.

Table 3.2 Comparison of system constants for eight surfactant-bound monolithic columns of different chain length, head group and linker.

monomer	**e**	**s**	**a**	**b**	**v**	**c**	r^2	***n***
AAOCL	1.3567	-0.6714	-0.9477	2.0583	0.8931	-1.8845	0.985	31
SE	0.09614	0.01144	0.02323	0.21002	0.23885	0.11625		
AADCL	1.7301	-0.4681	-0.8953	2.2301	0.346	-0.3219	0.996	31
SE	0.06516	0.0067	0.01109	0.09419	0.01362	0.01588		
AADoCL	1.9878	-0.1909	-0.8052	2.9129	0.2435	-1.5251	0.975	31
SE	0.12641	0.00657	0.01742	0.21509	0.21853	0.09428		
monomer	**e**	**s**	**a**	**b**	**v**	**c**	r^2	***n***
AADCA	1.08837	-0.2056	-0.9749	1.8411	0.98046	-1.1185	0.984	31
SE	0.09805	0.01164	0.0227	0.22874	0.24347	0.1185		
AADCV	1.43045	-0.0933	-0.7036	2.0417	0.72428	-1.691	0.992	31
SE	0.13024	0.00676	0.01729	0.23654	0.22499	0.09705		
monomer	**e**	**s**	**a**	**b**	**v**	**c**	r^2	***n***

AAUL	1.57148	-0.1394	-0.2159	2.974	0.48473	-1.7844	0.995	31
SE	0.08013	0.00566	0.0103	0.1055	0.1088	0.0483		
AAUA	1.33867	-0.1223	-0.2405	2.78226	0.88067	-2.08	0.988	31
SE	0.12058	0.00975	0.02112	0.25623	0.31647	0.08258		
AAUV	1.75949	-0.0699	-0.203	2.84954	0.54756	-1.9214	0.979	31
SE	0.16017	0.00566	0.0161	0.26501	0.29245	0.06		

SE: standard error; r^2: regression coefficient; n: number of achiral solutes in the regression.

3.4.2.1 Coefficient c

Under a closer look into every coefficient, the coefficient *c* is an independent system parameter and not solute related. Instead, *c* is related to column phase ratio and varies with column nature and experiment temperature.[4] As for all CSP, the coefficient c is negative, which means for any solutes, all eight stationary phase is less retentive than other CSP stationary with positive c value. As c value does not count in solute selectivity, it will not be further discussed.

3.4.2.2 Coefficient a

Coefficient *a* represents the interaction of H-bond basic character, which shows the second greatest variation among all coefficients, indicating high basic capability of the column structure.

3.4.2.3 Coefficient b

The coefficient *b* is the largest positive coefficient and bonding between acidic solutes and surfactant carbonyl group attached to the hydrocarbon chain as amide or carbamate spacer, which is related to the basic character of solute (B descriptor). With most polar interactions, the solutes favor the stationary phase.

3.4.2.4 Coefficient e and s

The *e* and *s* coefficients link the polarizability and dipole dipole interaction contributing to the selectivity. A negative value of *s* represents for the negative contributes of dipole-dipole interaction between the solutes and stationary phase. Thus, ompared to stationary phase, the solutes favors mobile phase.

3.4.2.5 Coefficient v

The cavity formation and disperation interaction, coefficient v, is the third most significant parameter contributing to retention. As for different head group monomer, the head group alanine, valine and leucine has an increasing molecular volume, which will effect on the polymer structure of monolith. One can observe that as the head group volume increases, the coefficient *v* decrease, which may be because that the smaller head group could form the proper cavity for the achiral solute. The relatively small *v* value is because all the solutes in this study does not have a large range of atom numbers, which reduced the influence of molecular volume.

3.4.3 Comparision of coefficient values

The three most significant coefficient appear to be *"b" "e"* and *"v"*. The bar plots comparing the effect of chain length, head group and linker type for system constant is shown in Figure 3.5. In the comparison of solutes between each columns, one could found with the increasing of monomer chain length from 8-12, the e-coefficient increased from 1.36 to 1.98, which means the interactions between π and n electrons is a leading interaction when the chain length is longer. As the monomer changed among alanine, leucine and valine, *a* and *b* values has a great change (23% and 21%), which is mainly because the monomer head group structure varied, leading to the hydrogen-bonding interaction change. When the crosslinker changes from methylene group to oxygen atom attached to carbonyl, the hydrophobicity of the stationary phase changed and the *e*-coefficient also decreased. Because *b, e* and *v* are three most significant contributor to retention, the discussion here is organized accordingly after constructing plots as suggested above.

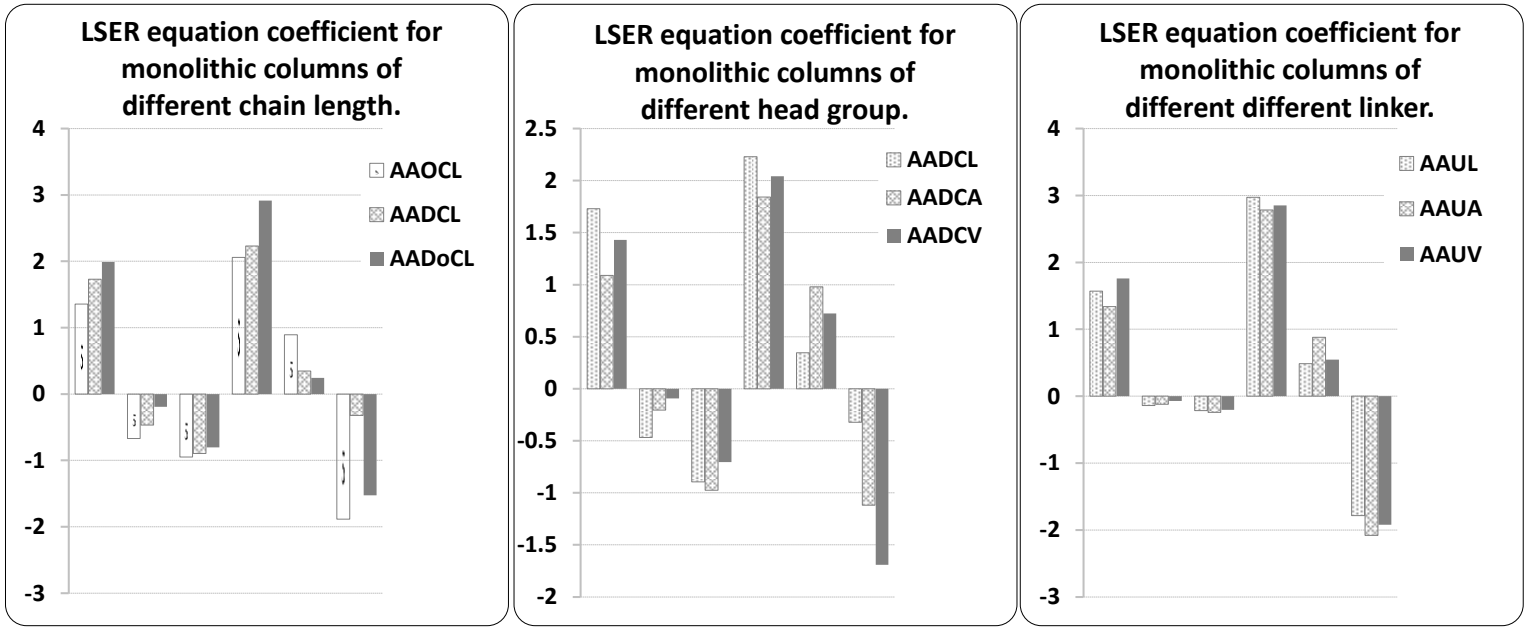

Figure 3.5 Bar plots showing system constants for eight surfactant-bound monolithic columns of different chain length, head group and different linker.

3.4.4 Test Compounds of Chiral LSERs Equation

A set of 42 chiral compounds were chosen to be tested on poly-AADCL-co-EDMA monolithic column. Out of all chiral compounds, seventeen chiral solutes were selected because they showed some degree of enantioseparation, including pindolol, metoprolol, cateolol, alprenolol, oxprenolol, atenolol, propranolol, pseudoephedrine, ephedrine, methylephedrine, norphenylephedrine, norepinephrine, benzoin, verapamil, nefopam, hexobarbital and terbutaline. The retention factor, selectivity and resolution are shown in Table 3.3.

Table 3.3 Resolution, selectivity and retention factors of chiral compounds separated on poly (AADCL-co-EDMA) monolith column.

Compounds	***Rs***	***Selectivity α***	***k_1®***	***k_2®***	***predicted k****
Pindolol	0.42	1.0123	2.60	2.69	3.0716
Cateolol	0.33	1.0211	0.75	0.76	2.8412
Alprenolol	0.94	1.1126	1.04	1.08	1.2236
Oxprenolol	1.12	1.2122	0.74	0.77	1.0671
Atenolol	0.91	1.0231	1.04	1.12	1.2896
Ephedrine	1.51	1.2342	1.04	1.09	1.2686
Benzoin	0.25	1.0124	0.04	0.17	1.5590
Verapamil	1.32	1.2144	0.46	1.09	1.2710
Nefopam	1.22	1.2078	0.51	1.78	0.9850
Hexobarbital	1.35	1.2122	0.06	0.59	0.9670
Terbutaline	1.51	1.3294	0.76	0.77	0.9490
Metoprolol	0.21	1.0241	2.04	**2.08**	**2.0839**
Pseudoephedrine	1.45	1.2901	1.35	**1.74**	**1.7413**

Methylephedrine	1.22	1.1450	1.35	**1.55**	**1.5455**
Propranolol	1.25	1.0841	2.33	**2.52**	**2.5245**
Norepinephrine	0.91	1.0725	1.35	**1.45**	**1.4476**
Norphenylephedrine	1.26	1.4551	0.86	**1.25**	**1.2518**

® $k_{1\ and}$ k_2 are obtained from experiment, as described in Step 3 of Figure 3.5; * Predicted k was calculated as described in Step 2 of Figure 3.6.

3.4.5 LSER Study of the Enantiomer-AADCL Interactions

To To generation the chiral LSERs equation, one need to first build the LSERs model based on the experimental *k*' and solutes descriptors of achiral compounds, which is shown in Table 3.2. Second, the predicted log*k*' value will be calculated by using the LSERs model equation and chiral solutes descriptor. After that, one need to compare the predicted logk_2' with the experimental logk_2'. If the predicted k and experimental k value matches, the first enantiomer would be consider to have a different set of coefficient. If there are six chiral solutes, which matches the predicted logk_2' with the experimental logk_2', it would be possible to calculate out another LSERs equation with first eluted enantiomer. By using Eq. 2, the *logα* could be concluded and all Δx terms could be determined.

After the test of all 17 chiral compounds, a set of experiment were performed with the same solutes and mobile phase but bare silica column. The corrected retention factor were calculated to eliminate the influence of ionic interaction. A detailed procedure to determine the coefficient value of chiral LSER is shown in Figure 3.6. Propranolol, pseudoephedrine, methylephedrine, norphenylephedrine, norepinephrine, metoprolol were found to match the predicted logk_2' with the experimental logk_2'.

Step 1

Build the LSER model based on the experimental *k'* and solutes descriptors of achiral compounds with SAS software.*

↓

log*k'=-0.3219+1.7301E+0.3460V-0.4680S-0.8953A+2.2301B*

Step 2

Using the LSER model equation to calculate the log *k'* of chiral solutes with known solute descriptors.

↓

e.g. insert the solute descriptors in the equation in step 1, the log of predicted retention factor. Fore example, pseudoephedrine log *k'*=0.2405, thus for pseudoephedrine , the predicted retention factor *k'*=1.7412

Step 3

Run the chiral compounds on the column and compare the predicted log *k'* with the experimental l*og k'*.

↓

For pseudoephedrine, experimental retention factor k_1 =1.35 and k_2=1.74 ; experimental k_2 =predicted k_2

Step 4

Screen more chiral compounds; For compounds experimental k_2 =predicted k_2 , collect all the experimental k_1 values; With known chiral solutes descriptor, generate the LSER equation with SAS.

↓

Six chiral solutes (propranolol, pseudoephedrine, ethylephedrine, norphenylephedrine, norepinephrine, metoprolol) with known descriptors (A, B, E, S,V) and experimental k1 was used to calculate the coefficient a1, b1, e1, s1, v1 from LSER,

log k_1'=-0.4521+1.6011E+0.3310V-0.4795S-0.9142A+2.1042B

Step 5

Use equation *logα= log k_2 –log k_1 = ΔeE+ΔsS+ΔaA+ΔbB+ΔvV =(a_2-a_1)A+(b_2-b_1)B+(e_2-e_1)E+(s_2-s_1)S+(v_2-v_1)V+c_2-c_1;* a_1, b_1, e_1, s_1, v_1 and c_1 are obtained from Step 4; a_1, b_1, e_1, s_1, v_1 and c_1 are obtained from Step 4; ; a_2, b_2, e_2, s_2, v_2 and c_2 are obtained from Step 1;.

↓

Log α= 0.129E+0.0114S+0.0171A+0.1259B+0.015V+0.1302

Figure 3.6 The procedure of enantioselectivity prediction using LSER model. * The experiment was based on poly (AADCL-co-EDMA) monolith column.

A new set of LSERs coefficient were generated and all Δx terms were calculated as shown in Table 3.4. Among all six parameters, e and b coefficient has the greatest value, suggesting Interactions between π and n electrons and hydrogen-bonding interaction with basic solutes are the dominating interactions for chiral recognition.

Table 3.4 Comparison of coefficient values of LSER equation on first and second eluted enantiomers.

	e	***s***	***a***	***b***	***v***	***c***
$logk_1$	1.6011	-0.4795	-0.9124	2.1042	0.331	-0.4521
** $logk_2$	1.7301	-0.4681	-0.8953	2.2301	0.346	-0.3219
	Δe	Δs	Δa	Δb	Δv	Δc
$log\alpha$	0.129	0.0114	0.0171	0.1259	0.015	0.1302

** coefficient values e_2, s_2, a_2, b_2, and v_2 from step 1 discussed in Figure 3.6;

A new set of LSERs coefficient were generated and all Δx terms were calculated as shown in Table 3.4. Among all six parameters, e and b coefficient has the greatest value, suggesting Interactions between π and n electrons and hydrogen-bonding interaction with basic solutes are the dominating interactions for chiral recognition.

Table 3.5 lists the A–V solute descriptors for the representative six enantiomers. By setting six simultaneous equation in LSER to obtain the equation for first eluting enantiomer, the retention factor and selectivity would be obtained. Six chiral solutes (propranolol, pseudoephedrine, ethylephedrine, norphenylephedrine, norepinephrine, metoprolol) with known descriptors (A, B, E, S,V) and experimental k_1 was used to calculate the coefficient a_1, b_1, e_1, s_1, v_1 from LSER.

Table 3.5 LSER solute descriptors of six molecular enantiomers *.

	E	*S*	*A*	*B*	*V*	r^2	SE
Metoprolol	0.320	1.133	0.610	0.297	1.450	0.955	0.042
Pseudoephedrine	0.310	0.118	0.780	0.114	1.410	0.986	0.023
Methylephedrine	0.290	0.249	1.020	0.196	1.310	0.965	0.027
Propranolol	0.320	0.250	1.090	0.299	1.440	0.963	0.026
Norepinephrine	0.260	0.185	1.210	0.345	1.210	0.972	0.024
Norphenylephedrine	0.320	0.138	1.210	0.300	1.210	0.963	0.023

When screening the chral compounds and compare the experimental retention factor with the predicted retention factor, three different cases were observed. Case (i) the retention factors predicted by LSER matches the first eluting enantiomer retention factor; Case (ii) the LSER predicted retention factors matches the second eluting enantiomer retention factor; Case (iii) the LSER predicted retention factors did not correspond to either enantiomer. From retention mechanical, it can be illustrated that that in Case (i), the chiral stationary phase has overall attractive enantioselective interactions with the second enantiomer; in Case (ii), the mobile phase has overall attractive enantioselective interactions with the first enantiomer; in Case (iii), enantioselective interactions of the chiral stationary phase are with both enantiomers. The matched retention factor compounds are shown in Figure 3.6

Table 3.6 LSER data for five components of enantioselectivity factors and enantioselectivity.

	ΔeE	ΔsS	ΔaA	ΔbB	ΔvV	*Predicted log*α[I]	*Predicted* α	Experimental α
Metoprolol	0.041	0.013	0.01	0.037	0.022	0.00847	1.020	1.024
Pseudoephedrine	0.04	0.001	0.013	0.014	0.021	0.11024	1.289	1.290
Methylephedrine	0.037	0.003	0.017	0.025	0.02	0.05997	1.148	1.145
Propranolol	0.041	0.003	0.019	0.038	0.022	0.03402	1.082	1.084
Norepinephrine	0.034	0.002	0.021	0.043	0.018	0.03104	1.074	1.073
Norphenylephedrine	0.041	0.002	0.021	0.038	0.018	0.16241	1.454	1.455

[I] Calculated from LSER equation (2), $\log\alpha = \log k_2 - \log k_1 = \Delta eE + \Delta sS + \Delta aA + \Delta bB + \Delta vV$.

The chiral separation for the matched six enantiomers are shown in Figure 3.7. The resolution and selectivity factor are listed in the figure. Although for the enantiomers, the resolution values vary from 0.21 to 1.45, they could still be inserted into the LSER equation and the linearity is from 0.955 to 0.986, shown in Table 3.5

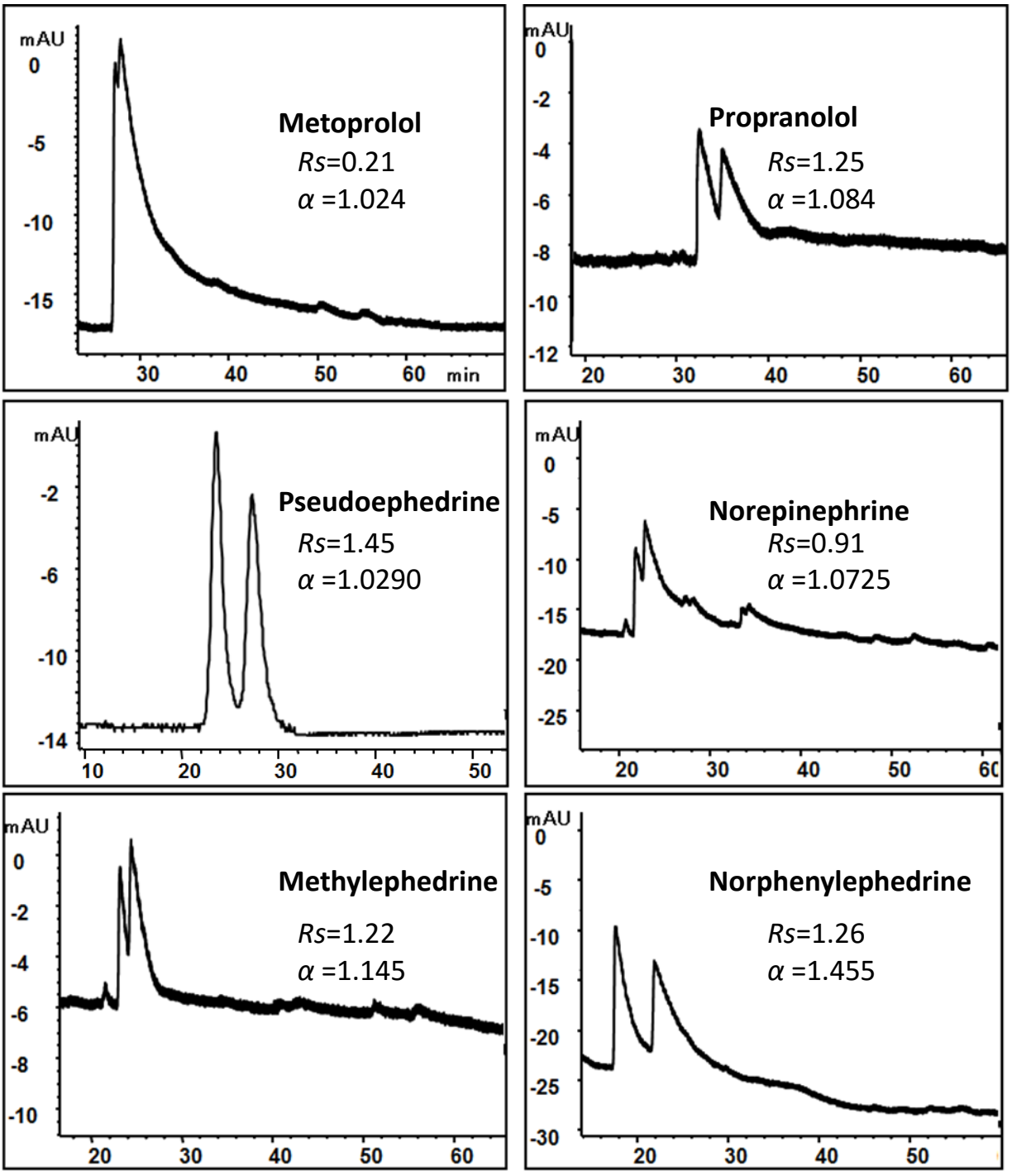

Figure 3.7 Chiral separation on poly-AADCL-co-EDMA monolithic column.

Knowing the A–V solute descriptors (Table 3.5, top) and the coefficient a-v are obtained as shown in Figure 3.4, it is easily to calculate Δ*xX terms* as shown in Table 3.6. A visual radar plot could

help us to understand the interactions and enantioselectivity between the CSP and solutes, as shown in Figure 3.8 easily obtained. The five terms of Eq. (2) form a branch of a star in Figure 3.8. This representation clearly show the strong positive contribution of the *e* term, the weak contribution of the *s* term and also, the significant contribution of the *b* term. All six radar plots showing the similar trending with the strong contribution *e* and weak contribution *s*. Also, the term b is the second contributed item, except for pseudoephedrine, due to the lower descriptor B.

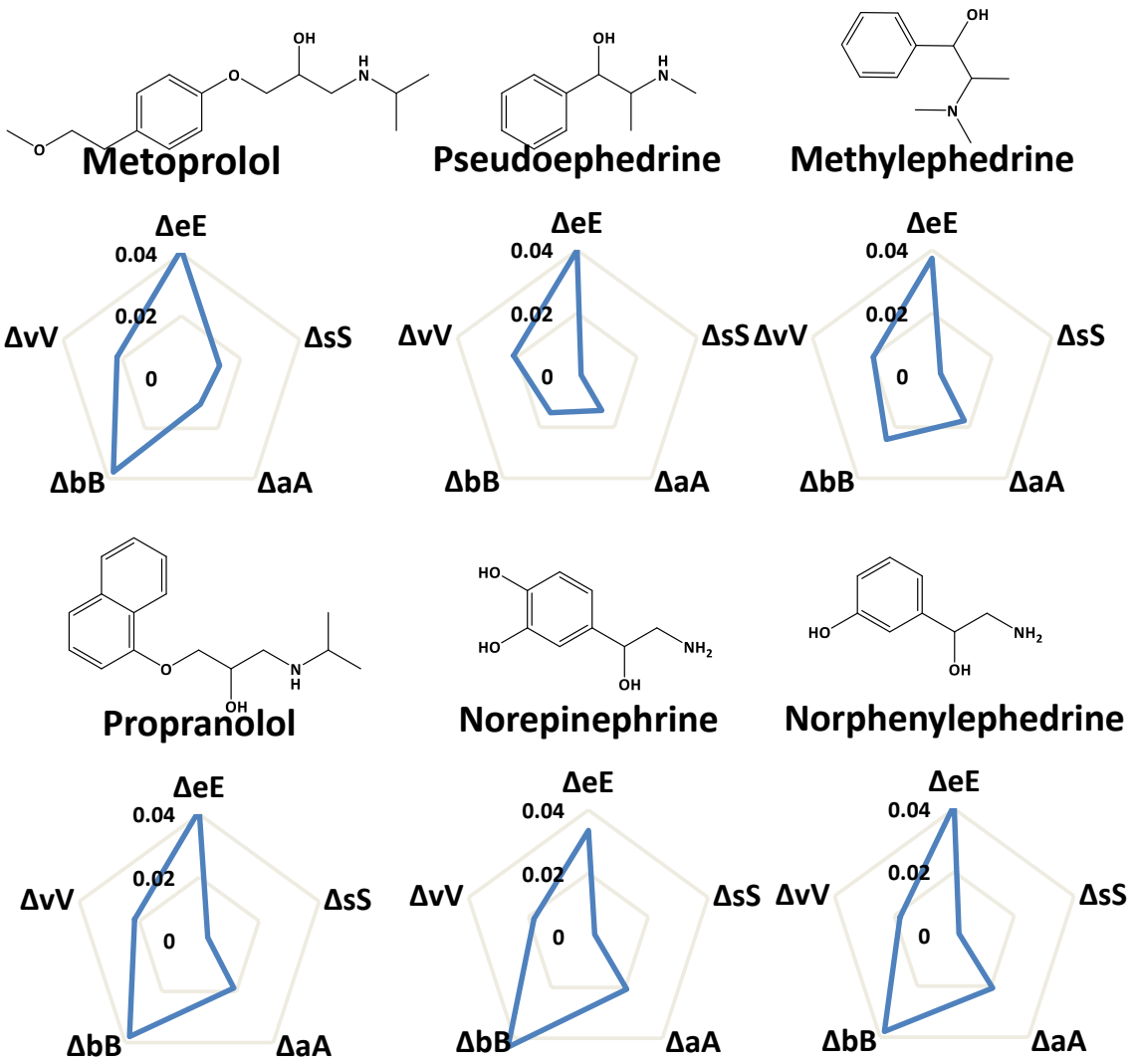

Figure 3.8 . Radar plots showing the five components of the enantioselectivity factors of molecular enantiomers separated on poly-(AADCL-co-EDMA) monolith.

3.5 Conclusion

LSERs studies can give the insight into chiral recognition when enantiomer get separated on the monolithic the CSP. It was found the enantiomers behavior on the same CSP are different and two sets of LSER coefficient could be generated. In addition, interactions between π and n electrons and hydrogen-bonding interaction with basic solutes are the dominating interactions for chiral

recognition. Thus, one could expect a set of enantiomer with higher n electrons and high hydrogen bonding accepting ability would have higher enantioselectivity potential.

References

(1) Szepesy, L. *J. Chromatogr. A* **2002**, *960*, 69-83.

(2) McGowan, J. C. *Recueil des Travaux Chimiques des Pays-Bas* **1956**, *75*, 193-208.

(3) Chen, L.-M.; Liu, X.; Jiang, S.-X. *Fenxi Huaxue* **2009**, *37*, 255-258.

(4) Berthod, A.; Mitchell, C. R.; Armstrong, D. W. *J Chromatogr A* **2007**, *1166*, 61-69.

(5) Mitchell, C. R.; Armstrong, D. W.; Berthod, A. *J Chromatogr A* **2007**, *1166*, 70-78.

(6) Blackwell, J. A.; Waltermire, R. E.; Stringham, R. W. *Enantiomer* **2001**, *6*, 353-367.

(7) He, J.; Wang, X.; Morrill, M.; Shamsi, S. A. *Analytical chemistry* **2012**, *84*, 5236-5242.

(8) West, C.; Guenegou, G.; Zhang, Y.; Morin-Allory, L. *J Chromatogr A* **2011**, *1218*, 2033-2057.

(9) Lu, Y.; Shamsi, S. A. *Journal of Chromatographic Science* **2014**, *52*, 1109-1120.

(10) Badaloni, E.; Barbarino, M.; Cabri, W.; D'Acquarica, I.; Forte, M.; Gasparrini, F.; Giorgi, F.; Pierini, M.; Simone, P.; Ursini, O.; Villani, C. *J Chromatogr A* **2011**, *1218*, 3862-3875.

(11) Akbay, C.; Shamsi, S. A. *Electrophoresis* **2004**, *25*, 635-644.

(12) Akbay, C.; Shamsi, S. A. *Electrophoresis* **2004**, *25*, 622-634.